Bioorganic & Medicinal Chemistry 17 (2009) 2461–2475

Contents lists available at ScienceDirect

Bioorganic & Medicinal Chemistry

journal homepage: www.elsevier.com/locate/bmc

Synthesis and evaluation of imidazole–dioxolane compounds as selective heme oxygenase inhibitors: Effect of substituents at the 4-position of the dioxolane ring

Jason Z. Vlahakis [a], Maaike Hum [b], Mona N. Rahman [c], Zongchao Jia [c], Kanji Nakatsu [b], Walter A. Szarek [a,*]

[a] Department of Chemistry, Queen's University, Kingston, Ontario, Canada K7L 3N6
[b] Department of Pharmacology & Toxicology, Queen's University, Kingston, Ontario, Canada K7L 3N6
[c] Department of Biochemistry, Queen's University, Kingston, Ontario, Canada K7L 3N6

ARTICLE INFO

Article history:
Received 23 October 2008
Revised 30 January 2009
Accepted 31 January 2009
Available online 12 February 2009

Keywords:
Heme oxygenase
Imidazole–dioxolane inhibitors
Carbon monoxide
Heme
Molecular modeling

ABSTRACT

Several imidazole–dioxolane compounds were synthesized and evaluated as novel inhibitors of heme oxygenase (HO). These compounds, which include a series of substituted thiophenol and substituted phenol derivatives of (2*R*,4*S*)-2-[2-(4-chlorophenyl)ethyl]-2-[(1*H*-imidazol-1-yl)methyl]-4-[(phenylsulfanyl)methyl]-1,3-dioxolane hydrochloride (**3**), in addition to smaller functionalized derivatives, continue our structure–activity studies by exploration of the aminothiophenol region ('northeastern region') in our original target structure azalanstat (**1**). In vitro, most of the compounds in this series were found to be highly potent inhibitors of the stress-induced isozyme HO-1 and the constitutive isozyme HO-2, showing only moderate selectivity for HO-1. Nevertheless, a few of the compounds displayed higher selectivity toward HO-1. None of the compounds having a larger appendage in the northeastern region were inhibitors of CYP2E1, whereas a compound having a relatively small fluorine substituent in this region did inhibit CYP2E1; all of the compounds tested exhibited high inhibitory potency against CYP3A1/3A2.

© 2009 Elsevier Ltd. All rights reserved.

1. Introduction

The heme oxygenase (HO) system comprises two active isozymes, namely, HO-1 (inducible) and HO-2 (constitutive), and is involved in the biotransformation of heme into biliverdin, releasing carbon monoxide (CO) and ferrous iron (Fe^{2+}) in the process (Fig. 1).[1,2] The cellular regulatory actions of CO have recently been acknowledged widely,[3–5] and the use of HO inhibitors as pharmacological tools is critical in the elucidation of the physiological functions of the CO/HO system and related physiological pathways. Such inhibitors may be useful when investigating the role of HO-1 in various clinical situations such as: a protective effect in acute renal failure,[6] its role in the response to cardiovascular-system injuries,[7] a role in neurodegenerative diseases,[8] and its promotion of the growth of solid tumors.[9] Owing to the lack of selectivity of first-generation HO inhibitors, which are metalloporphyrin-based, our laboratory has been concerned with the design of new HO inhibitors that are not based on the porphyrin nucleus, having the objective of obtaining more-selective HO inhibitors. The discovery[2] of imidazole-based azalanstat (**1**) as a lead compound allowed the design of novel, more-selective inhibitors of these

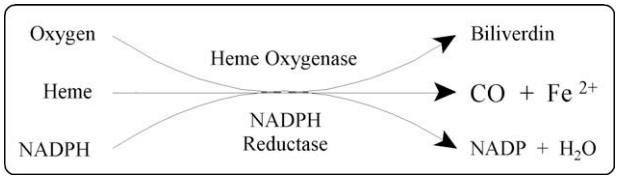

Figure 1. The oxidative degradation of heme in the CO/HO pathway.

enzymes; azalanstat itself is a potent inhibitor of HO-1 and HO-2 and has minimal effects on other enzymes usually inhibited by metalloporphyrins such as nitric oxide synthase (NOS) or soluble guanylyl cyclase (sGC).[10] Our initial structure–activity study of a series of twelve azalanstat analogs[11] showed that different degrees of selectivity in the inhibition of HO-1 relative to HO-2 could be achieved by modifying the position of the amino functionality on the aminothiophenol moiety in the northeastern region of azalanstat (**1**) or by modifying the diastereomeric configuration of the substituents attached to the dioxolane ring in the central region (Fig. 2). Thus, we embarked on a mission to systematically explore the various regions of the azalanstat structure with a view of designing highly isozyme-selective HO inhibitors.

The present work focuses initially on the investigation of the structure–activity relationship brought about by subtle modifica-

* Corresponding author. Tel.: +1 613 533 2643; fax: +1 613 533 6532.
E-mail address: szarekw@chem.queensu.ca (W.A. Szarek).

0968-0896/$ - see front matter © 2009 Elsevier Ltd. All rights reserved.
doi:10.1016/j.bmc.2009.01.078

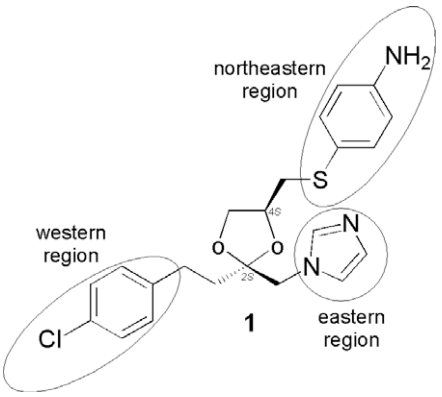

Figure 2. Topological representation of the azalanstat molecule **1**.

tions to the northeastern (NE) region of azalanstat, namely, replacing the aminothiophenol moiety by other substituted thiophenol or substituted phenol moieties (see Fig. 3). For proper comparison we chose to adopt only the (2*R*,4*S*) configuration of the dioxolane ring system as a template, as this configuration was shown[11] to produce both potent and selective HO-1 inhibitors. Further investigations[12] showed that the complete removal of the aminothiophenol moiety (replacement by hydrogen) in the NE region produced a methyl-terminated series of compounds (including **2**) having enhanced selectivity for the inhibition of HO-1 relative to HO-2. Thus, we also studied structure–activity relationships that result from replacing the aminothiophenol moiety by smaller functional groups such as halo, hydroxy, methoxy, thiomethoxy, cyano, thiocyanato, azido, amino, and imidazolyl.

2. Results and discussion

2.1. Synthesis

In an effort to fully evaluate the importance that structural features in the northeastern region have on HO-1 and HO-2 activities, a simple synthetic strategy was devised to produce many substituted analogs of the parent compound **3**, a compound that simply contains a benzenethiol moiety in the northeastern region, an optimized (2*R*,4*S*) dioxolane ring configuration, and the rest of the azalanstat structure including the 4-chlorophenethyl motif in the western region and the 1-substituted imidazole moiety in the eastern region. Each of these regions is being studied systematically, and is the subject of a separate publication; for example, the results of our efforts in optimizing the western region have been published,[13] and work on the eastern region is in progress.

Following an approach similar to that previously reported,[11] our synthetic strategy involved utilizing the diastereomeric tosylate intermediate **4**, and generating analogs by modification in the last synthetic step. As shown in Scheme 1, the arylthio and alkylthio analogs of **3** (namely, **5**–**19**) were synthesized by a nucleophilic displacement reaction on tosylate **4** using the appropriately substituted thiophenol or alkanethiol in acetone/Cs_2CO_3 in a manner similar to that previously performed using acetone/K_2CO_3.[11] Aryloxy analogs of **3** (namely, **20**–**29**) were also synthesized by nucleophilic displacement reactions on tosylate **4** using the appropriately substituted phenol in *N*,*N*-dimethylformamide (DMF)/Cs_2CO_3; higher reaction temperatures and longer reaction times were required. In a similar approach, other northeastern-region analogs (namely, **30**–**37**) were synthesized by nucleophilic displacement reactions on tosylate **4** using various nucleophiles, as outlined in Scheme 2. The hydroxy-terminated derivative **30** was obtained from **4** using potassium hydroxide/lithium hydroxide in DMF. Similarly, treatment of **4** with sodium methoxide in DMF gave the methoxy-containing derivative **37**. The thiomethoxide derivative **31** was prepared using sodium thiomethoxide in acetone/Cs_2CO_3 in a manner similar to that previously performed using acetone/K_2CO_3.[11] Displacement by chloride to afford compound **34** was achieved using lithium chloride in DMF.[14] Displacement by fluoride to afford compound **32** was achieved using tetra-*n*-butylammonium fluoride in THF. The displacement reaction on tosylate **4** using sodium azide in DMF[15] afforded compound **35**. The azide **35** was fully reduced to the amine **36** (the chloro group was also reduced) using ammonium formate and 10% Pd/C catalyst in methanol (catalytic hydrogen transfer conditions) by the published procedure.[16] The diimidazole compound **33** was obtained by treatment of **4** with an excess of imidazole in DMF.

Since all of these reactions were performed on only one purified diastereomeric tosylate, only one diastereomeric product was produced in each case; these imidazole-containing compounds were isolated/characterized/evaluated in their hydrochloride or dihy-

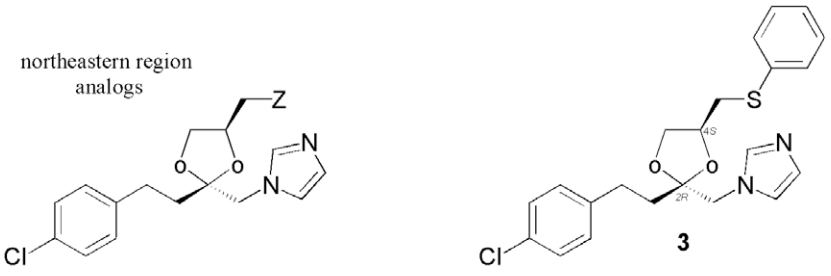

Figure 3. General structure of northeastern region analogs and one such compound (**3**).

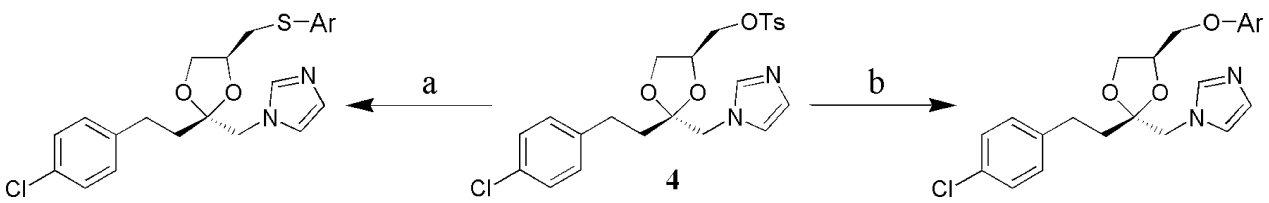

Scheme 1. Reagents and conditions: (a) ArSH (or RSH), Cs_2CO_3, acetone, reflux, 6 h; (b) ArOH, Cs_2CO_3, DMF, 90 °C, 8 h.

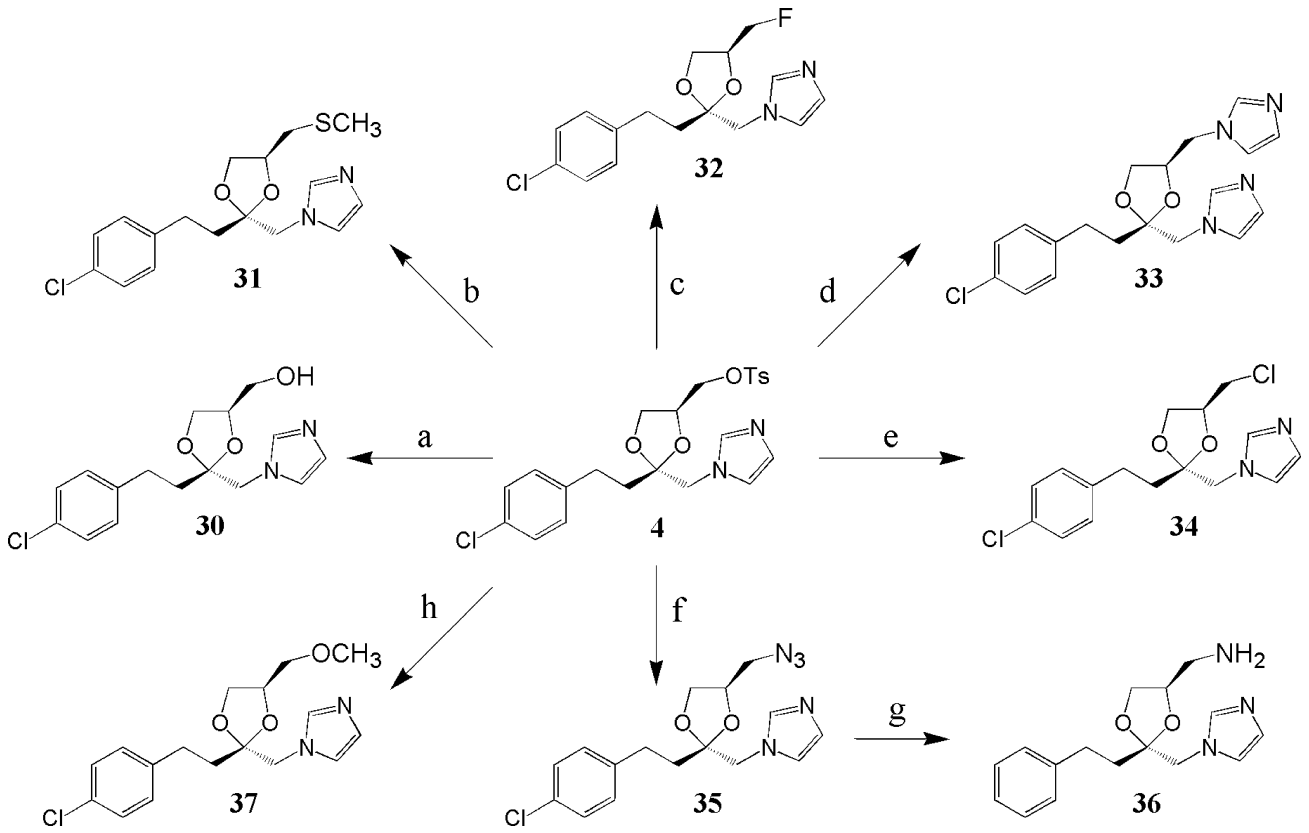

Scheme 2. Reagents and conditions: (a) KOH, LiOH, DMF, 120 °C, 9 h; (b) $NaSCH_3$, Cs_2CO_3, acetone, reflux, 6 h; (c) Bu_4NF, THF, reflux, 18.5 h; (d) imidazole, DMF, 110 °C, 30 h; (e) LiCl, DMF, 110 °C, 1 h; (f) NaN_3, DMF, 110 °C, 2 h; (g) NH_4OCOH, 10% Pd/C, CH_3OH, reflux, 3 h; (h) $NaOCH_3$, DMF, 120 °C, 7 h.

drochloride salt forms of the structures shown. Following these strategies, 31 new, northeastern-region analogs were synthesized and evaluated for their ability to inhibit HO-1 and HO-2.

2.2. Biological evaluation

As described in Section 4, the compounds in Table 1 were screened for evidence of their ability to inhibit HO-1 and HO-2 using an in vitro assay for HO in which heme was presented to the enzyme complexed with albumin. HO-1 was obtained from rat spleen and HO-2 was obtained from rat brain as the microsomal fractions prepared by differential centrifugation; the dominance of HO-1 protein in the rat spleen and HO-2 protein in the rat brain, has been documented.[17–19,10] These particular microsomal preparations were selected in order to use the most native (i.e., closest to in vivo) forms of HO, that is, those being most relevant to anticipated whole-animal studies. We appreciate that pure forms of HO can be obtained but these enzymes are membrane-free and truncated. The data from biological screening assays are presented in Table 1; the ratio of IC_{50} values measured for HO-2 and HO-1 for each compound is shown in the fifth column, and is used as the index of selectivity for HO-1 compared to HO-2.

Previous work[11] on azalanstat and its structural analogs (including **5**–**7**) showed potent inhibition of both HO-1 and HO-2 which appeared to be dependent on the position of the amino group on the thiophenol moiety. Further exploration[12] revealed that the aminothiophenol moiety is not an absolute requirement for HO-inhibition because its removal enhanced the selectivity for HO-1 inhibition (compound **2**). We concluded that the aminothiophenol group (or other group in the analogous northeastern position) may be an important factor for recognition in the HO-2 system. Thus, we chose to investigate this region further by synthesizing many NE-region analogs because this approach had the potential to identify inhibitors selective for HO-2. However, HO-2 selectivity was not achieved, as most of the compounds tested were potent inhibitors of both HO-1 and HO-2, always showing less activity toward HO-2 (Table 1). In contrast to the metalloporphyrins which show modest selectivity toward HO-2,[20] all of the imidazole–dioxolane compounds studied herein appear to be selective for HO-1.

Our systematic investigation of analogs of **3** originally focused on the modification of the benzenethiol moiety; incorporating other substituted thiophenol appendages. As shown in Table 1, nearly all of the compounds in the thiophenol-containing series exhibit high inhibitory potency against HO-1 (13 out of the 16 compounds exhibit IC_{50} values of less than 5 μM for HO-1). Although the HO-2 inhibitory activity of these compounds is consistently lower, only 5 of the 16 compounds (namely, **3**, **5**, **6**, **16**, and **17**) show selectivity indexes greater than 10. Although not as striking as with our most-selective inhibitor to date (compound **2**, selectivity index ~381), a few of the new compounds show modest selectivity for HO-1. For instance, representative activity–inhibitor concentration curves showing the difference in potency toward HO-1 (rat spleen) and HO-2 (rat brain) activity exhibited by compound **17** are shown in Figure 4. The IC_{50} was 0.9 ± 0.1 μM for HO-1 (rat spleen) and 30 ± 4 μM for HO-2 (rat brain), with a modest selectivity index of 30. For comparison, representative activity–inhibitor concentration curves showing the difference in potency toward HO-1 (rat spleen) and HO-2 (rat brain) activity exhibited by the essentially non-selective HO inhibitor **19** are shown in Figure 5.

With respect to potency and selectivity, similar results (Table 1) were noted with the analogous phenol-containing derivatives; 8 of the 10 compounds exhibit IC_{50} values of less than 5 μM for HO-1,

Table 1
Inhibitory potency and selectivity of thiophenol- and phenol-containing imidazole–dioxolanes against the activity of HO-1 and HO-2[a]

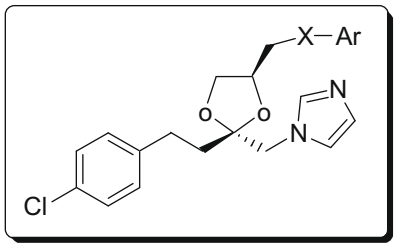

Compound	X–Ar	IC_{50} (μM) rat spleen (HO-1)	IC_{50} (μM) rat brain (HO-2)	Selectivity index IC_{50} (HO-2)/IC_{50} (HO-1)
3	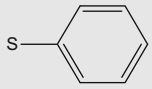	1.03 ± 0.07	34 ± 12	*33*
5[b]	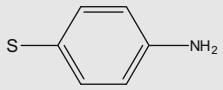	0.33 ± 0.07[b]	8 ± 1[b]	*20*
6[b]	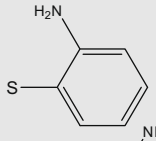	4 ± 2[b]	42 ± 28[b]	*10*
7[b]	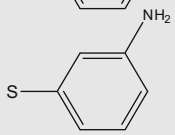	4 ± 2[b]	6 ± 1[b]	*2*
8	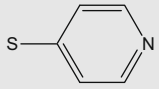	25 ± 5	69 ± 8	*2.8*
9[c]	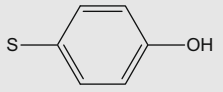	1.59 ± 0.03	7 ± 2	*4*
10	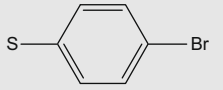	2.1 ± 0.9	2.4 ± 0.1	*1.1*
11	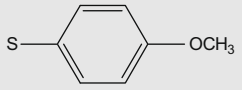	0.7 ± 0.3	2.5 ± 0.4	*4*
12	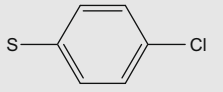	2.8 ± 0.4	12 ± 5	*4.3*
13	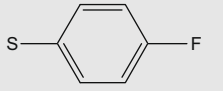	2.2 ± 0.2	5 ± 4	*2*
14	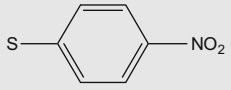	6 ± 2	19 ± 2	*3*
15	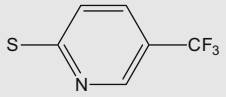	2.1 ± 0.6	16 ± 8	*7.6*

Table 1 (*continued*)

Compound	X–Ar	IC_{50} (μM) rat spleen (HO-1)	IC_{50} (μM) rat brain (HO-2)	Selectivity index IC_{50} (HO-2)/IC_{50} (HO-1)
16[d]	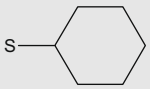	0.94 ± 0.09	13 ± 2	*14*
17	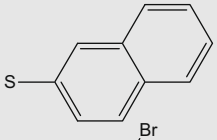	0.9 ± 0.1	30 ± 4	*30*
18	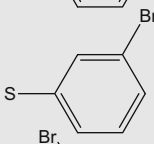	5 ± 2	22 ± 9	*4*
19	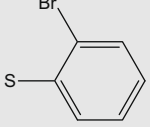	6 ± 1	12.3 ± 0.5	*2*
20	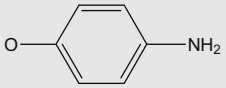	1.4 ± 0.3	13 ± 4	*9.3*
21	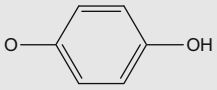	1.8 ± 0.5	7.1 ± 0.7	*3.9*
22	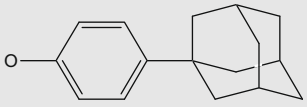	> 100	> 100	—
23	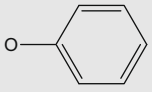	0.59 ± 0.04	1.6 ± 0.3	*2.7*
24	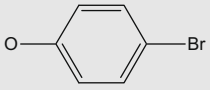	3.5 ± 0.2	22 ± 8	*6.3*
25		0.28 ± 0.01	0.5 ± 0.2	*2*
26	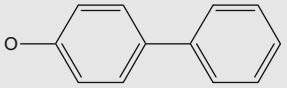	2 ± 1	43 ± 3	*20*
27	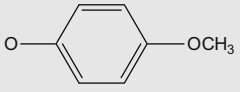	1.33 ± 0.03	19 ± 7	*14*
28		9 ± 3	15 ± 4	*2*
29	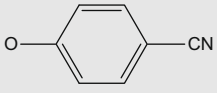	0.67 ± 0.02	1.7 ± 0.2	*2.5*

[a] Assays were performed as indicated in Section 4. Data represent mean IC_{50} values ± standard deviation of replicate experiments. All imidazole–dioxolane compounds were evaluated as the hydrochloride or dihydrochloride salt of the structure shown.

[b] Biological data and compound synthesis originally published in Ref. 11; biological data included in this table for comparison.

[c] Compound synthesis originally published in Ref. 29.

[d] The cyclohexylsulfanyl-containing derivative **16** is included in this table for comparison.

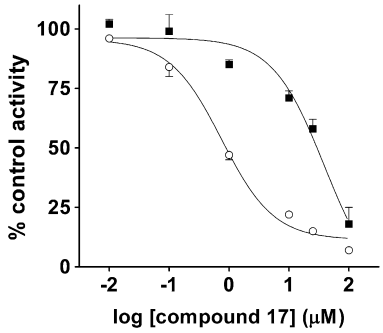

Figure 4. Inhibition of HO-1 and HO-2 by a thionaphthyl-substituted imidazole–dioxolane (compound **17**). Enzyme activities were determined as described in Section 4. Activity (ordinate) is expressed as a percentage of the control with no inhibitor present, mean ± SD. The values on the abscissa represent the log of the inhibitor concentration in μM. ○, HO-1 (rat spleen microsomes). ■, HO-2 (rat brain microsomes).

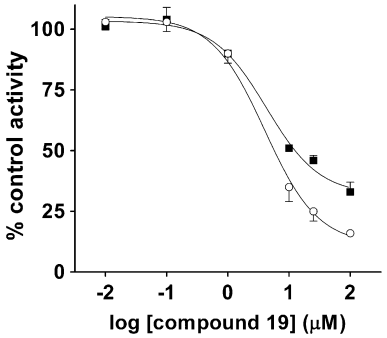

Figure 5. Inhibition of HO by compound **19**—lack of isozyme selectivity. Enzyme activities were determined as described in Section 4. ○, HO-1. ■, HO-2.

but only 2 of the 10 compounds (namely, **26** and **27**) show selectivity indices greater than 10. From this study, the effect of the replacement of sulfur by oxygen on biological activity is not immediately apparent. No trend in potency and/or selectivity is noticed when comparing appropriate compound pairs such as **3**/**23**, **9**/**21**, **10**/**24**, **11**/**27**, and **13**/**25**.

It appears that the addition of an extra aromatic ring system (compared to that of **3**) to the northeastern region (as in compounds **17** and **26**) is well tolerated, and even beneficial to attain higher selectivity for HO-1. However, the system can be extended too far, as noticed with the incorporation of the 4-adamantyl moiety to produce compound **22**, a compound inactive toward both HO-1 and HO-2. It is interesting to note that, of the compounds in the thiophenol/phenol series, 4 of the 6 most selective compounds (namely, **3**, **16**, **17**, and **26**) all contain hydrocarbon moieties in the northeastern region (as in the case of our most-selective inhibitor **2**). Thus, further modification to include more non-polar functionality in the NE-region may be worth exploring.

The compounds in Table 2 possess more-dramatic changes to the azalanstat skeleton in the NE region, and represent our efforts at the incorporation of relatively small, polar functionality to this area. Although the drastic structural changes did have significant impact on activity/selectivity, we observed similar results as with the thiophenol/phenol-containing derivatives; the compounds are HO-1 selective, with a few derivatives showing modest selectivity. For instance, representative activity–inhibitor concentration curves showing a difference in potency toward HO-1 (rat spleen) and HO-2 (rat brain) activity exhibited by compound **34** are shown in Figure 6. The IC_{50} was 3.5 ± 0.1 μM for HO-1 (rat spleen) and 122 ± 30 μM for HO-2 (rat brain), with a modest selectivity index

Table 2
Inhibitory potency and selectivity of various imidazole–dioxolanes, having a small substituent at the 4-position of the dioxolane ring, against the activity of HO-1 and HO-2[a]

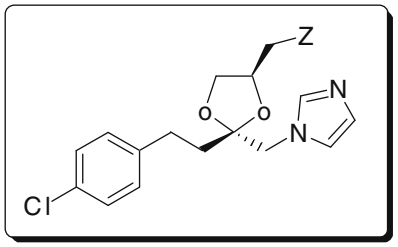

Compound	Z	IC_{50} (μM) rat spleen (HO-1)	IC_{50} (μM) rat brain (HO-2)	Selectivity index IC_{50} (HO-2)/IC_{50} (HO-1)
2[b]	H	0.8 ± 0.2[b]	305 ± 25[b]	~*381*[b]
30	OH	12 ± 2	>100	*>8*
31	SCH_3	9 ± 2	19 ± 7	*2*
32	F	1.20 ± 0.01	4.4 ± 0.4	*3.7*
33		10 ± 6	26 ± 3	*2.6*
34	Cl	3.5 ± 0.1	122 ± 30	*35*
35	N_3	3.6 ± 0.2	38 ± 5	*11*
36[c]	NH_2	21 ± 3	>100	*>5*
37	OCH_3	1.73 ± 0.01	3.3 ± 0.9	*1.9*

[a] Assays were performed as indicated in Section 4. Data represent mean IC_{50} values ± standard deviation of replicate experiments. All imidazole–dioxolane compounds were evaluated as the hydrochloride or dihydrochloride salt of the structure shown.

[b] Biological data and compound synthesis originally published in Ref. 12; biological data included in this table for comparison.

[c] The chlorine atom in the 4-position of the phenyl ring in the general structure is replaced by a hydrogen atom.

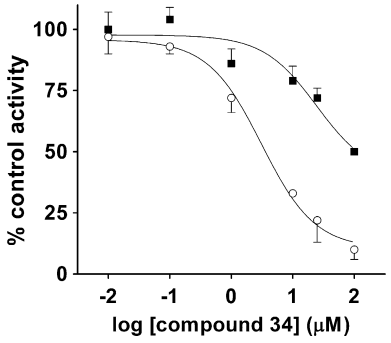

Figure 6. HO isozyme selectivity exhibited by a compound having a small substituent at the 4-position of the dioxolane ring. Representative activity–inhibitor concentration curves for the inhibition of HO-1 and HO-2 by compound **34**. Enzyme activities were determined as described in Section 4. ○, HO-1. ■, HO-2.

of 35. Because of the wide variety of functionality incorporated into these series of compounds, structure–activity relationships are difficult to formulate. Nonetheless, most of the compounds in Table 2 have lower potency against both HO-1 and HO-2 compared to the compounds in Table 1 which have larger groups in the northeastern region. As with all of the imidazole–dioxolane compounds studied thus far, HO-1 selectivity is apparent; the inhibitors having smaller groups in the northeastern region show mild to modest selectivity, although never achieving the isozyme-specific characteristic of compound **2**. The thiomethyl-containing analog **31** and the diimidazole compound **33** show little preference for HO-1 inhibition, while the halogen-containing derivatives **32** and **34** are quite selective.

We have addressed also the issue of selectivity with respect to other hemoproteins such as cytochromes P450[21] (CYP). The in vitro screening of our compounds for the inhibition of CYP is necessary because cytochromes P450 are responsible for the metabolism of many drugs used in therapy and as experimental tools. As shown in Table 3, all of the 11 compounds tested exhibit high inhibitory potency against CYP3A1/3A2. Interestingly, with the exception of compound **32**, none of the compounds were inhibitors of CYP2E1. It is noteworthy that the majority of compounds in Table 3 have large appendages in the NE region and did not inhibit CYP2E1, whereas compound **32** contains only a relatively small F substituent in this region, and did inhibit CYP2E1. These results are consistent with our previous investigations,[10,12] in that analogs devoid of large NE-region substituents were potent inhibitors of CYP2E1. Thus, for compounds having large NE-region substituents, although there was a low selectivity for HO-1 over HO-2, there was a noticeable selectivity for CYP3A1/3A2 over CYP2E1. For instance, representative activity–inhibitor concentration curves in Figure 7 showed a difference in potency toward CYP2E1 (IC_{50} > 100 μM) and CYP3A1/3A2 (IC_{50} 7 ± 4 μM) activity by compound **8**. We plan to continue our study of selectivity to include other hemoenzymes, namely, soluble guanylyl cyclase (sGC) and nitric oxide synthase (NOS); we have reported previously[12] that similar imidazole–dioxolane compounds (analogs of **2**) are extremely weak inhibitors of sGC and neuronal NOS.

Table 3
Inhibition of CYP2E1 and CYP3A1/3A2 by various imidazole–dioxolanes[a]

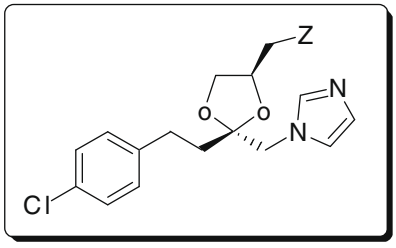

Compound	Z	IC_{50} (μM) (CYP2E1)	IC_{50} (μM) (CYP3A1/3A2)
3	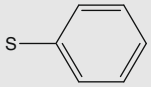	>100	2 ± 1
8	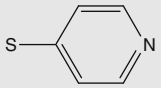	>100	7 ± 4
9	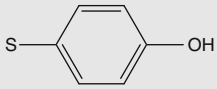	>100	1.4 ± 0.2
10	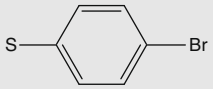	>100	2.1 ± 0.4
16	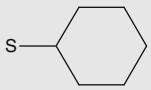	>100	2.8 ± 0.8
17	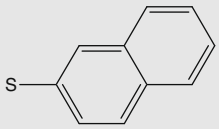	>100	1.8 ± 0.4
21	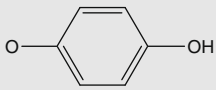	>100	2.0 ± 0.8
24	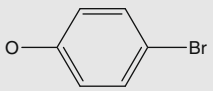	>100	3.4 ± 0.6
29	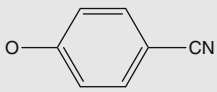	>100	6.9 ± 0.5
31	SCH_3	>100	2.2 ± 0.6
32	F	3.6 ± 0.2	4 ± 1

[a] Assays were performed as indicated in Section 4. Data represent mean IC_{50} values ± standard deviation of replicate experiments. All of the imidazole–dioxolane compounds were evaluated as the hydrochloride or dihydrochloride salts of the structure shown.

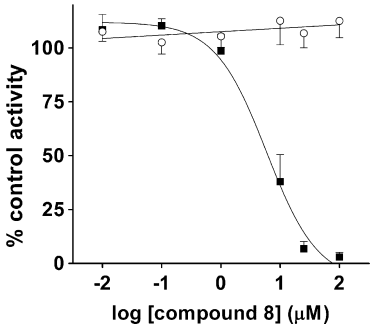

Figure 7. Representative activity–inhibitor concentration curves for the inhibition of CYP2E1 and CYP3A1/3A2 by compound **8**—compound **8** inhibited CYP3A1/3A2 but not CYP2E1. Enzyme activities were determined as described in Section 4. ○, CYP2E1. ■, CYP3A1/3A2.

Most of our synthetic modifications to the NE region led to compounds active against both HO-1 and HO-2 but lacking strikingly high selectivity. Inhibitors with high potency against HO-2 were always even more potent against HO-1. Thus, at least for this diastereomeric series, it seems unlikely that HO-2 selectivity will be achieved by such modifications in this region. Conversely, coupled with our knowledge[12] that removal of the northeastern portion leads to highly selective HO-1 inhibitors, it seems unlikely that extremely selective inhibitors of HO-1 will be developed from simple modifications to appendages in the NE region (the hydrocarbon substituents appear to be an exception, and may be worthwhile exploring).

2.3. Modeling of HO–inhibitor complexes

In an effort to rationalize some of our experimental observations, a modeling study was performed based on the X-ray crystallographic structural data of hHO-1 in complex with analogous inhibitors. We have previously published[22] the structure of hHO-1 in which azalanstat had been docked (AUTODOCK version 3.0) to show a secondary hydrophobic pocket into which the northeastern region of the molecule fit. Using this model as a guide, inhibitor **3** was placed (CCP4: XFit) in the inhibitor binding site of hHO-1 (Fig. 8A). The structure of hHO-1 utilized was based on the X-ray crystallographic structure of hHO-1 in complex with 1-(adamantan-1-yl)-2-(1*H*-imidazol-1-yl)ethanone (PDB 3CZY) from which the inhibitor had been omitted. This template was the same as that utilized for the original automated docking of azalanstat to hHO-1.

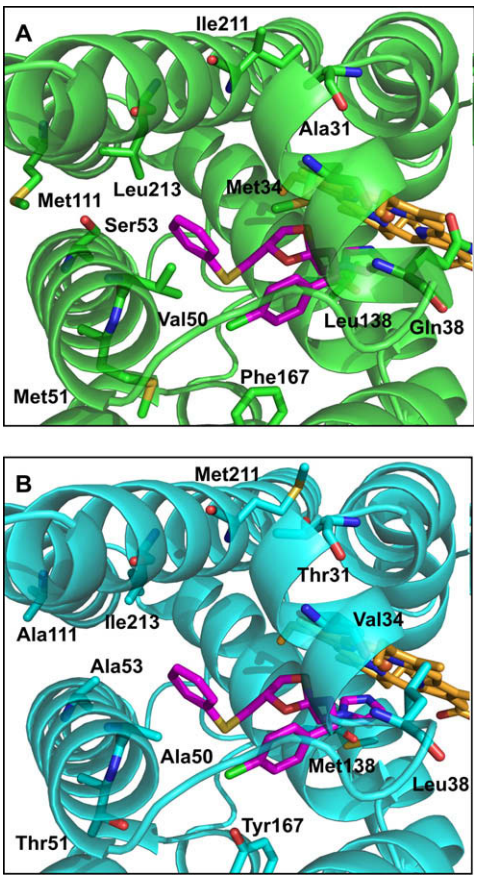

Figure 8. (A) Model of inhibitor **3** (magenta) in complex with hHO-1. (B) Model of inhibitor **3** (magenta) in complex with hHO-1 in which the residues involved in inhibitor binding have been changed to those of hHO-2. The modified residues are indicated and labeled accordingly. Heme is colored orange.

For comparison with the hHO-2 system, residues within the inhibitor binding site of hHO-1 were mutated to those of hHO-2[23] (i.e., Met34→Val, Leu213→Ile, Ser53→Ala, Val50→Ala, Met111→Ala, Ile211→Met, Ala31→Thr, Gln38→Leu, Phe167→Tyr, and Met51→Thr, Leu138→Met) (Fig. 8B). Since the structure of the inhibitor compounds in this study differ only in the northeastern region, only residues in the putative secondary hydrophobic pocket were analyzed.

Previous crystallographic studies[22] have demonstrated that when hHO-1 binds an inhibitor, there is substantial movement in the distal helix as well as, to a lesser extent, in the proximal pocket to open up the heme-binding pocket in order to accommodate the inhibitor. Indeed, the presence of the putative secondary hydrophobic pocket was apparent only in the crystal structure of hHO-1 in complex with the bulky 1-(adamantan-1-yl)-2-(1*H*-imidazol-1-yl)ethanone[22] and not in the native structure,[24,25] or in the structure of rat HO-1 in complex with 2-[2-(4-chlorophenyl)ethyl]-2-[(1*H*-imidazol-1-yl)methyl]-1,3-dioxolane.[26] Thus, the heme-binding pocket of the native (truncated) hHO-1 structure could not be used in our modeling studies as the pocket was not large enough. Given that the structures of hHO-1 and hHO-2 are so similar, we anticipate that hHO-2 would have to undergo similar changes in structure (i.e., expansion) to accommodate the inhibitor. Since an X-ray crystallographic structure of hHO-2 in complex with an inhibitor is unavailable, we changed residues in the inhibitor-bound hHO-1 binding pocket with residues of hHO-2 to effectively approximate the inhibitor-bound binding pocket of hHO-2. With respect to the residues that differ between hHO-1 and hHO-2 in the secondary hydrophobic pocket, it would appear that the substitutions in hHO-2 would result in a larger hydrophobic pocket (see Fig. 8). Thus, the shorter residues in hHO-2 would be farther away from the phenyl group in the northeastern region of inhibitor **3**. For example, replacement of the Leu213 in hHO-1 by the corresponding Ile of hHO-2 increases the distance between the phenyl ring of inhibitor **3** and the residue from 3.6 Å to 4.4 Å. Replacement of Val50 by Ala would also increase the distance between residue and inhibitor by ~0.8 Å (3.1–3.9 Å). Although the distance from the Ser53 of hHO-1 to inhibitor **3** would be similar if substituted with Ala (4.5 Å), the hydroxyl group of Ser53 in the hHO-1 model would be close enough to be within van der Waals contact of the inhibitor if it were rotated toward the hydrophobic pocket. Moreover, this may also provide a site for hydrogen-bond interactions with a suitable inhibitor, a situation which would not be present in hHO-2. The replacement of Met34 by Val would increase the distance to the phenyl group in the northeastern region of compound **3** by ~2 Å; the distance between this residue and the phenyl moiety increased from 4.4 to 6.7 Å. In general, the slightly larger, secondary hydrophobic pocket of hHO-2 may result in decreased contacts with the northeastern portion of our inhibitors; this may explain the general selectivity observed for HO-1 over HO-2 with these compounds.

As previously noted, some of the most selective compounds for HO-1 in this series contain hydrocarbon moieties in the northeastern region. Conversely, compounds having electronegative substituents in this region would impart a negative-charge distribution in an area (the secondary hydrophobic pocket) which is generally hydrophobic; accordingly, a general decrease in potency was observed with each of HO-1 and HO-2 for most compounds not containing non-polar moieties in the northeastern region. Although one can infer, based on the previous X-ray crystallographic structures of the native[24,25] and inhibitor-bound HO-1 (both rat[26] and human[22]), that there may be some flexibility in the secondary hydrophobic pocket, there are length limitations. For example, compound **22** possesses an extended northeastern region that contains, in addition to the phenyl group, a bulky adamantyl terminus. This group is clearly too large and bulky to fit into the pocket owing to steric hindrance, an observation reflected by the lack of inhibitory activity toward HO we observed using this compound.

It should be noted, that the hHO crystal structures solved to date do not represent the full-length enzymes found in vivo.[23–25] Both proteins contain a membrane-binding tail, while hHO-2 also contains three heme-regulatory motifs which have been removed for crystallization.[23,27] One should not overlook the possibility that these absent regions may have some influence on the binding/potency of inhibitors.

3. Conclusions

We have synthesized several compounds that express moderate selectivity as inhibitors of HO-1 relative to HO-2. In particular, compounds **2**, **3**, **5**, **6**, **16**, **17**, **26**, **27**, **34**, and **35** are noteworthy for moderately high potency and selectivity toward HO-1. In addition, we have synthesized potent but non-selective inhibitors of HO-2 such as **10**, **11**, **23**, **25**, **29**, **32**, and **37.** Our systematic investigation of the northeastern section of the lead compound azalanstat has shed light on our overall regional study, suggesting that we focus our modifications elsewhere. Although synthetically demanding, these compounds are anticipated to become useful tools in elucidating the physiological roles of HO and carbon monoxide in mammalian and other biological systems, as regards both HO-1 and HO-2. These novel compounds might also have useful therapeutic applications, either alone or in conjunction with other novel agents.

4. Experimental

4.1. General

The ^1H and ^{13}C NMR spectra were recorded on a Bruker Avance 400 MHz spectrometer in CD_3OD or D_2O. The signals owing to residual protons in the deuterated solvents were used as internal standards in the measurement of ^1H NMR spectra. Chemical shifts (δ) are reported in ppm downfield from tetramethylsilane.[28] Carbon chemical shifts are given relative to CD_3OD: $\delta = 49.00$ or $CDCl_3$: $\delta = 77.16$. High-resolution electrospray mass spectra were recorded on an Applied Biosystems/MDS Sciex QSTAR XL spectrometer with an Agilent HP1100 Cap-LC system. Samples were run in 50% aqueous MeOH at a flow rate of 6 μL/min. Elemental analyses were performed by MHW Laboratories (Phoenix, AZ, USA). Melting points were determined on a Mel-Temp II melting point apparatus and are uncorrected. Optical rotations were measured using an Autopol® II automatic polarimeter for solutions in a 1-dm cell at rt. Column chromatography was performed on Silicycle silica gel (230–400 mesh, 60 Å). Analytical thin-layer chromatography was performed using glass- or aluminum-backed Silica Gel 60 F_{254} plates (Silicycle, Quebec City, QC, Canada). Plates were viewed under UV light or by charring after spraying with phosphomolybdic acid (PMA) in EtOH.

4.2. Materials

Dexamethasone-5 was obtained from Vetoquinol Canada Inc, Lavaltrie, QC, Canada. Erythromycin, *p*-nitrophenol, β-NADPH, ethylenediamine tetraacetic acid disodium salt (EDTA), and 70% perchloric acid were obtained from Sigma Chemical Company, St. Louis, MO, USA. Acetone, glycerol, ammonium acetate, glacial acetic acid, KCl, KH_2PO_4, and KOH were obtained from Fisher Scientific Ltd, Ottawa, ON, Canada. (2*R*,4*S*)-2-[2-(4-Chlorophenyl)ethyl]-2-[(1*H*-imidazol-1-yl)methyl]-4-[(*p*-toluenesulfonyloxy)methyl]-1,3-dioxolane (**4**) and compounds **5**–**7** were prepared according to the published procedures.[11] The synthesis of compound **9** has been published in a previous communication.[29] All other chemical reagents were obtained from Sigma–Aldrich and used without prior purification.

4.3. Representative procedure for the displacement of the *p*-toluenesulfonyloxy group in compound 4 using thiophenol-containing nucleophiles

4.3.1. (2*R*,4*S*)-2-[2-(4-Chlorophenyl)ethyl]-2-[(1*H*-imidazol-1-yl)methyl]-4-[(phenylsulfanyl)methyl]-1,3-dioxolane hydrochloride (3)

Under a N_2 atmosphere, a mixture of (2*R*,4*S*)-2-[2-(4-chlorophenyl)ethyl]-2-[(1*H*-imidazol-1-yl)methyl]-4-[(*p*-toluenesulfonyloxy)methyl]-1,3-dioxolane (**4**)[11] (178 mg, 0.37 mmol), benzenethiol (82 mg, 0.74 mmol, 2 equiv), and cesium carbonate (241 mg, 0.74 mmol, 4 equiv) in acetone (7 mL) was heated at reflux temperature with stirring for 6 h. The solids were removed by filtration, and washed with hot acetone and then with hot ethyl acetate. The filtrate was concentrated, and the residue ($R_f \approx 0.2$ in EtOAc) purified by flash chromatography on silica gel (EtOAc) to give the free base (150 mg, 0.36 mmol, 98%) as an oil. To a solution of the oil in warm 2-propanol (2 mL) was added a solution of 37% aqueous HCl (50 mg, 0.51 mmol, 1.4 equiv) in 2-propanol (2 mL). The mixture was concentrated and dried under high vacuum. The residue was dissolved in 2-propanol (0.5 mL), the solution cooled in the freezer, and then a few drops of Et_2O were added and the product allowed to crystallize overnight. The solid was removed by filtration and washed with Et_2O. High-vacuum drying left **3** (150 mg, 0.33 mmol, 89%) as a white solid: mp 134–135 °C; $R_f = 0.24$ (EtOAc); $[\alpha]_D^{23}$ −8.2 (*c* 1.7 in CD_3OD); ^1H NMR (400 MHz, CD_3OD): δ 1.97 (t, $J = 8.4$ Hz, 2H), 2.66–2.84 (m, 2H), 3.09 (dd, $J = 13.8$, 5.8 Hz, 1H), 3.19 (dd, $J = 14.0$, 4.8 Hz, 1H), 3.66–3.75 (m, 2H), 4.00–4.90 (m, 1H), 4.45 (s, 2H), 7.16 (d, $J = 8.4$ Hz, 2H), 7.20–7.42 (m, 7H), 7.50 (br s, 1H), 7.58 (br s, 1H), 8.92 (br s, 1H); ^{13}C NMR (100 MHz, CD_3OD): δ 29.8, 36.7, 39.2, 54.7, 70.9, 78.0, 109.9, 120.5, 125.0, 127.7, 129.5, 130.2, 130.9, 131.0, 132.8, 136.8, 137.7, 141.4; HRMS (ESI) $[M-Cl]^+$ Calcd for $C_{22}H_{24}ClN_2O_2S$: 415.1247. Found: 415.1233. Anal. Calcd for $C_{22}H_{24}Cl_2N_2O_2S$: C, 58.54; H, 5.36; N, 6.21. Found: C, 58.44; H, 5.28; N, 6.06.

4.4. Characterization of the new compounds synthesized following the representative procedure described above for compound 3, as outlined in Scheme 1

4.4.1. (2*R*,4*S*)-2-[2-(4-Chlorophenyl)ethyl]-2-[(1*H*-imidazol-1-yl)methyl]-4-[(pyridin-4-ylsulfanyl)methyl]-1,3-dioxolane dihydrochloride (8)

Hygroscopic white solid in 76% yield from **4**[11]: $[\alpha]_D^{24}$ +22.3 (*c* 2.0 in CD_3OD); ^1H NMR (400 MHz, CD_3OD): δ 1.93–2.05 (m, 2H), 2.65–2.82 (m, 2H), 3.45 (dd, $J = 14.2$, 5.8 Hz, 1H), 3.64 (dd, $J = 14.8$, 4.8 Hz, 1H), 3.87 (t, $J = 8.2$ Hz, 1H), 4.00–4.10 (m, 1H), 4.19 (dd, $J = 8.6$, 6.2 Hz, 1H), 4.47 (s, 2H), 7.14 (d, $J = 8.4$ Hz, 2H), 7.26 (d, $J = 8.4$ Hz, 2H), 7.59 (t, $J = 1.6$ Hz, 1H), 7.65 (t, $J = 1.6$ Hz, 1H), 7.90 (d, $J = 7.2$ Hz, 2H), 8.50 (d, $J = 6.4$ Hz, 2H), 8.99 (s, 1H); ^{13}C NMR (100 MHz, CD_3OD): δ 29.8, 33.8, 38.7, 54.3, 70.2, 76.7, 110.3, 120.7, 123.9, 125.1, 129.6, 130.9, 132.9, 137.8, 140.7, 141.1, 165.9; HRMS (ESI) $[M-Cl]^+$ Calcd for $C_{21}H_{23}ClN_3O_2S$: 416.1199. Found: 416.1183.

4.4.2. (2*R*,4*S*)-4-[(4-Bromophenylsulfanyl)methyl]-2-[2-(4-chlorophenyl)ethyl]-2-[(1*H*-imidazol-1-yl)methyl]-1,3-dioxolane hydrochloride (10)

White solid in 96% yield from **4**[11]: mp 141–142 °C; $R_f = 0.23$ (EtOAc); $[\alpha]_D^{22}$ −4.5 (*c* 0.9 in CD_3OD); ^1H NMR (400 MHz, CD_3OD): δ 1.95 (t, $J = 8.4$ Hz, 2H), 2.64–2.80 (m, 2H), 3.13 (dd, $J = 14.0$, 5.6 Hz, 1H), 3.19 (dd, $J = 14.0$, 5.2 Hz, 1H), 3.69–3.79 (m, 2H), 4.01–4.09 (m, 1H), 4.45 (s, 2H), 7.14 (d, $J = 8.4$ Hz, 2H), 7.26 (d, $J = 8.4$ Hz, 2H), 7.30 (d, $J = 8.8$ Hz, 2H), 7.45 (d, $J = 8.8$ Hz, 2H), 7.52 (br s, 1H), 7.59 (br s, 1H), 8.92 (br s, 1H); ^{13}C NMR (100 MHz, CD_3OD): δ 29.8, 36.6, 39.1, 54.6, 70.8, 78.0, 110.0, 120.6, 121.2, 125.1, 129.6, 131.0, 132.3, 132.9, 133.2, 136.6, 137.8, 141.3; HRMS (ESI) $[M-Cl]^+$ Calcd for $C_{22}H_{23}BrClN_2O_2S$: 493.0352. Found: 493.0336. Anal. Calcd for $C_{22}H_{23}BrCl_2N_2O_2S$: C, 49.83; H, 4.37; N, 5.28. Found: C, 50.52; H, 4.50; N, 4.66.

4.4.3. (2*R*,4*S*)-2-[2-(4-Chlorophenyl)ethyl]-2-[(1*H*-imidazol-1-yl)methyl]-4-[(4-methoxyphenylsulfanyl)methyl]-1,3-dioxolane hydrochloride (11)

Beige solid in 73% yield from **4**[11]: mp 139–140 °C; $R_f = 0.16$ (EtOAc); $[\alpha]_D^{22}$ −9.2 (*c* 0.9 in CD_3OD); ^1H NMR (400 MHz, CD_3OD): δ 1.95 (t, $J = 8.4$ Hz, 2H), 2.64–2.78 (m, 2H), 2.93 (dd, $J = 13.8$, 5.8 Hz, 1H), 3.07 (dd, $J = 13.8$, 5.0 Hz, 1H), 3.59–3.68 (m, 2H), 3.79 (s, 3H), 3.98–4.05 (m, 1H), 4.43 (s, 2H), 6.89 (d, $J = 8.8$ Hz, 2H), 7.17 (d, $J = 8.4$ Hz, 2H), 7.26 (d, $J = 8.4$ Hz, 2H), 7.36 (d, $J = 8.4$ Hz, 2H), 7.51 (br s, 1H), 7.58 (br s, 1H), 8.89 (br s, 1H); ^{13}C NMR (100 MHz, CD_3OD): δ 29.8, 38.9, 39.2, 54.7, 55.8, 71.0, 78.4, 109.8, 115.8, 120.7, 125.0, 126.6, 129.5, 131.0, 132.8, 134.8, 137.8, 141.4, 161.0; HRMS (ESI) $[M-Cl]^+$ Calcd for $C_{23}H_{26}ClN_2O_3S$: 445.1353. Found: 445.1362. Anal. Calcd for $C_{23}H_{26}Cl_2N_2O_3S$: C, 57.38; H, 5.44; N, 5.82. Found: C, 57.68; H, 5.73; N, 6.06.

4.4.4. (2*R*,4*S*)-2-[2-(4-Chlorophenyl)ethyl]-4-[(4-chlorophenylsulfanyl)methyl]-2-[(1*H*-imidazol-1-yl)methyl]-1,3-dioxolane hydrochloride (12)

White solid in 80% yield from **4**[11]: mp 128–129 °C; R_f = 0.20 (EtOAc); $[\alpha]_D^{22}$ −5.2 (*c* 0.8 in CD_3OD); ^1H NMR (400 MHz, CD_3OD): δ 1.96 (t, *J* = 8.4 Hz, 2H), 2.64–2.81 (m, 2H), 3.12 (dd, *J* = 14.2, 5.4 Hz, 1H), 3.19 (dd, *J* = 14.0, 5.2 Hz, 1H), 3.69–3.78 (m, 2H), 4.01–4.09 (m, 1H), 4.45 (s, 2H), 7.15 (d, *J* = 8.4 Hz, 2H), 7.26 (d, *J* = 8.4 Hz, 2H), 7.31 (d, *J* = 8.8 Hz, 2H), 7.37 (d, *J* = 8.4 Hz, 2H), 7.52 (br s, 1H), 7.59 (br s, 1H), 8.92 (br s, 1H); ^{13}C NMR (100 MHz, CD_3OD): δ 29.8, 36.8, 39.1, 54.6, 70.8, 78.0, 109.9, 120.6, 125.1, 129.6, 130.2, 131.0, 132.2, 132.9, 133.5, 135.9, 137.8, 141.3; HRMS (ESI) $[M-Cl]^+$ Calcd for $C_{22}H_{23}Cl_2N_2O_2S$: 449.0857. Found: 449.0851. Anal. Calcd for $C_{22}H_{23}Cl_3N_2O_2S$: C, 54.39; H, 4.77; N, 5.77. Found: C, 54.53; H, 4.71; N, 5.64.

4.4.5. (2*R*,4*S*)-2-[2-(4-Chlorophenyl)ethyl]-4-[(4-fluorophenylsulfanyl)methyl]-2-[(1*H*-imidazol-1-yl)methyl]-1,3-dioxolane hydrochloride (13)

Hygroscopic beige solid in 70% yield from **4**[11]: mp 112–113 °C; R_f = 0.25 (EtOAc); $[\alpha]_D^{24}$ −9.4 (*c* 1.9 in CD_3OD); ^1H NMR (400 MHz, CD_3OD): δ 1.96 (t, *J* = 8.4 Hz, 2H), 2.65–2.80 (m, 2H), 3.05 (dd, *J* = 14.0, 5.6 Hz, 1H), 3.15 (dd, *J* = 13.8, 5.0 Hz, 1H), 3.64–3.74 (m, 2H), 4.01–4.09 (m, 1H), 4.46 (s, 2H), 7.07 (∼t, *J* = 8.8 Hz, 2H), 7.17 (d, *J* = 8.4 Hz, 2H), 7.26 (d, *J* = 8.4 Hz, 2H), 7.44 (∼dd, *J* = 8.8, 5.2 Hz, 2H), 7.53 (br s, 1H), 7.60 (br s, 1H), 8.93 (br s, 1H); ^{13}C NMR (100 MHz, CD_3OD): δ 29.8, 38.0, 39.1, 54.6, 70.9, 78.1, 109.9, 117.1 (d, $^2J_{C-F}$ = 22.2 Hz), 120.6, 125.1, 129.5, 131.0, 132.0 (d, $^4J_{C-F}$ = 3.6 Hz), 132.8, 134.0 (d, $^3J_{C-F}$ = 8.0 Hz), 137.8, 141.3, 163.5 (d, $^1J_{C-F}$ = 44.5 Hz); ^{19}F NMR (376 MHz, CD_3OD): δ −118.1 (t, $^1J_{F-C}$ = 6.6 Hz); HRMS (ESI) $[M-Cl]^+$ Calcd for $C_{22}H_{23}ClFN_2O_2S$: 433.1153. Found: 433.1154. Anal. Calcd for $C_{22}H_{23}Cl_2FN_2O_2S$: C, 56.29; H, 4.94; N, 5.97. Found: C, 56.12; H, 5.04; N, 6.02.

4.4.6. (2*R*,4*S*)-2-[2-(4-Chlorophenyl)ethyl]-2-[(1*H*-imidazol-1-yl)methyl]-4-[(4-nitrophenylsulfanyl)methyl]-1,3-dioxolane hydrochloride (14)

Hygroscopic yellow solid in 55% yield from **4**[11]: mp moistens at 70 °C; R_f = 0.14 (EtOAc); $[\alpha]_D^{23}$ +8.9 (*c* 0.7 in CD_3OD); ^1H NMR (400 MHz, CD_3OD): δ 1.97 (t, *J* = 8.4 Hz, 2H), 2.64–2.81 (m, 2H), 3.30–3.41 (m, 2H), 3.80 (t, *J* = 8.2 Hz, 1H), 3.84–3.92 (m, 1H), 4.12 (dd, *J* = 8.0, 5.6 Hz, 1H), 4.45 (s, 2H), 7.12 (d, *J* = 8.4 Hz, 2H), 7.24 (d, *J* = 8.4 Hz, 2H), 7.52 (d, *J* = 9.2 Hz, 2H), 7.54 (br s, 1H), 7.62 (br s, 1H), 8.14 (d, *J* = 8.8 Hz, 2H), 8.94 (br s, 1H); ^{13}C NMR (100 MHz, CD_3OD): δ 29.8, 34.6, 39.0, 54.5, 70.6, 77.5, 110.1, 120.7, 124.9, 125.1, 128.1, 129.5, 130.9, 132.9, 137.8, 141.2, 146.8, 147.9; HRMS (ESI) $[M-Cl]^+$ Calcd for $C_{22}H_{23}ClN_3O_4S$: 460.1098. Found: 460.1075. Anal. Calcd for $C_{22}H_{23}Cl_2N_3O_4S$: C, 53.23; H, 4.67; N, 8.46. Found: C, 53.09; H, 4.70; N, 8.23.

4.4.7. (2*R*,4*S*)-2-[2-(4-Chlorophenyl)ethyl]-2-[(1*H*-imidazol-1-yl)methyl]-4-[{(5-trifluoromethyl)pyridin-2-ylsulfanyl}methyl]-1,3-dioxolane hydrochloride (15)

White solid in 90% yield from **4**[11]: mp 156–157 °C; $[\alpha]_D^{20}$ −24.2 (*c* 0.8 in CD_3OD); ^1H NMR (400 MHz, CD_3OD): δ 2.00 (t, *J* = 8.4 Hz, 2H), 2.69–2.88 (m, 2H), 3.48 (dd, *J* = 14.0, 6.0 Hz, 1H), 3.57 (dd, *J* = 14.0, 5.2 Hz, 1H), 3.77 (t, *J* = 8.4 Hz, 1H), 3.88–3.97 (m, 1H), 4.08 (dd, *J* = 8.4, 6.0 Hz, 1H), 4.47 (∼s, 2H), 7.19 (d, *J* = 8.4 Hz, 2H), 7.27 (d, *J* = 8.4 Hz, 2H), 7.45 (d, *J* = 8.4 Hz, 1H), 7.54 (br s, 1H), 7.62 (br s, 1H), 7.85 (dd, *J* = 8.6, 2.2 Hz, 1H), 8.68 (br s, 1H), 8.94 (br s, 1H); ^{13}C NMR (100 MHz, CD_3OD): δ 29.8, 32.3, 39.1, 54.6, 70.6, 77.7, 109.9, 120.6, 123.2, 123.9 (d, $^2J_{C-F}$ = 33.2 Hz), 125.1, 125.3 (q, $^1J_{C-F}$ = 271.0 Hz), 129.6, 130.9, 132.9, 134.4 (d, $^3J_{C-F}$ = 3.5 Hz), 137.8, 141.3, 147.2 (d, $^3J_{C-F}$ = 3.9 Hz), 164.6; ^{19}F NMR (376 MHz, CD_3OD): δ −64.6; HRMS (ESI) $[M-Cl]^+$ Calcd for $C_{22}H_{22}ClF_3N_3O_2S$: 484.1073. Found: 484.1056. Anal. Calcd for $C_{22}H_{22}Cl_2F_3N_3O_2S$: C, 50.78; H, 4.26; N, 8.07. Found: C, 50.59; H, 4.26; N, 7.97.

4.4.8. (2*R*,4*S*)-2-[2-(4-Chlorophenyl)ethyl]-4-[(cyclohexylsulfanyl)methyl]-2-[(1*H*-imidazol-1-yl)methyl]-1,3-dioxolane hydrochloride (16)

White solid in 81% yield from **4**[11]: mp 172–173 °C; R_f = 0.36 (free base, EtOAc); $[\alpha]_D^{23}$ −18.1 (*c* 0.4 in CD_3OD); ^1H NMR (400 MHz, CD_3OD): δ 1.20–1.40 (m, 5H), 1.58–1.68 (m, 1H), 1.71–1.82 (m, 2H), 1.90–2.00 (m, 2H), 2.00 (dd, *J* = 9.2, 7.6 Hz, 2H), 2.62–2.73 (m, 2H), 2.73–2.86 (m, 3H), 3.68–3.76 (m, 2H), 4.04–4.12 (m, 1H), 4.47 (s, 2H), 7.21 (d, *J* = 8.4 Hz, 2H), 7.28 (d, *J* = 8.4 Hz, 2H), 7.59 (∼t, *J* = 1.6 Hz, 1H), 7.64 (∼t, *J* = 1.6 Hz, 1H), 8.96 (br s, 1H); ^{13}C NMR (100 MHz, CD_3OD): δ 26.9, 27.0, 29.8, 33.0, 34.8, 34.9, 39.2, 45.3, peak under solvent, 54.7, 71.1, 79.1, 109.8, 120.6, 125.1, 129.6, 131.0, 132.9, 137.8, 141.4; HRMS (ESI) $[M-Cl]^+$ Calcd for $C_{22}H_{30}ClN_2O_2S$: 421.1716. Found: 421.1698. Anal. Calcd for $C_{22}H_{30}Cl_2N_2O_2S$: C, 57.76; H, 6.61; N, 6.12; S, 7.01. Found: C, 58.11; H, 6.70; N, 6.13; S, 6.79.

4.4.9. (2*R*,4*S*)-2-[2-(4-Chlorophenyl)ethyl]-2-[(1*H*-imidazol-1-yl)methyl]-4-[(naphthalen-2-ylsulfanyl)methyl]-1,3-dioxolane hydrochloride (17)

White solid in 90% yield from **4**[11]: mp 156–157 °C; R_f = 0.26 (free base, EtOAc); $[\alpha]_D^{24}$ −7.4 (*c* 0.5 in CD_3OD); ^1H NMR (400 MHz, CD_3OD): δ 1.94 (t, *J* = 8.4 Hz, 2H), 2.62–2.78 (m, 2H), 3.19–3.34 (m, 2H), 3.73–3.83 (m, 2H), 4.07 (dd, *J* = 7.2, 4.8 Hz, 1H), 4.43 (s, 2H), 7.08 (d, *J* = 8.4 Hz, 2H), 7.22 (d, *J* = 8.4 Hz, 2H), 7.38 (∼t, *J* = 1.6 Hz, 1H), 7.43–7.53 (m, 3H), 7.56 (∼t, *J* = 1.6 Hz, 1H), 7.75–7.88 (m, 4H), 8.90 (br s, 1H); ^{13}C NMR (100 MHz, CD_3OD): δ 29.8, 36.5, 39.2, 54.6, 70.9, 78.2, 109.9, 120.4, 125.0, 127.1, 127.9, 128.2, 128.6, 128.7, 128.8, 129.5, 129.7, 130.9, 132.8, 133.5, 134.4, 135.2, 137.7, 141.3; HRMS (EI) $[M-HCl]^+$ Calcd for $C_{26}H_{25}ClN_2O_2S$: 464.1325. Found: 464.1347. Anal. Calcd for $C_{26}H_{26}Cl_2N_2O_2S$: C, 62.27; H, 5.23; N, 5.59. Found: C, 62.16; H, 5.05; N, 5.53.

4.4.10. (2*R*,4*S*)-4-[(3-Bromophenylsulfanyl)methyl]-2-[2-(4-chlorophenyl)ethyl]-2-[(1*H*-imidazol-1-yl)methyl]-1,3-dioxolane hydrochloride (18)

White solid in 90% yield from **4**[11]: mp 128–129 °C; R_f = 0.32 (free base, EtOAc); $[\alpha]_D^{23}$ −6.7 (*c* 0.7 in CD_3OD); ^1H NMR (400 MHz, CD_3OD): δ 1.96 (t, *J* = 8.6 Hz, 2H), 2.65–2.79 (m, 2H), 3.14–3.25 (m, 2H), 3.70–3.82 (m, 2H), 4.07 (dd, *J* = 7.2, 4.8 Hz, 1H), 4.46 (s, 2H), 7.14 (d, *J* = 8.0 Hz, 2H), 7.19–7.25 (m, 1H), 7.26 (d, *J* = 8.4 Hz, 2H), 7.33–7.39 (m, 2H), 7.54 (br s, 1H), 7.56 (t, *J* = 1.8 Hz, 1H), 7.60 (br s, 1H), 8.93 (br s, 1H); ^{13}C NMR (100 MHz, CD_3OD): δ 29.8, 36.2, 39.1, 54.6, 70.7, 78.0, 110.0, 120.6, 123.8, 125.1, 129.0, 129.5, 130.4, 131.0, 131.7, 132.6, 132.9, 137.8, 139.9, 141.3; HRMS (ESI) $[M-Cl]^+$ Calcd for $C_{22}H_{23}BrClN_2O_2S$: 493.0352. Found: 493.0333. Anal. Calcd for $C_{22}H_{23}BrCl_2N_2O_2S$: C, 49.83; H, 4.37; N, 5.28. Found: C, 49.95; H, 4.58; N, 5.19.

4.4.11. (2*R*,4*S*)-4-[(2-Bromophenylsulfanyl)methyl]-2-[2-(4-chlorophenyl)ethyl]-2-[(1*H*-imidazol-1-yl)methyl]-1,3-dioxolane hydrochloride (19)

Hygroscopic white solid in 100% yield from **4**[11]: R_f = 0.28 (free base, EtOAc); $[\alpha]_D^{22}$ −14.4 (*c* 0.6 in CD_3OD); ^1H NMR (400 MHz, CD_3OD): δ 1.97 (t, *J* = 8.6 Hz, 2H), 2.67–2.80 (m, 2H), 3.14–3.25 (m, 2H), 3.73–3.80 (m, 2H), 4.04–4.11 (m, 1H), 4.46 (s, 2H), 7.11 (∼td, *J* = 7.8, 1.6 Hz, 1H), 7.16 (d, *J* = 8.4 Hz, 2H), 7.25 (d, *J* = 8.4 Hz, 2H), 7.34 (∼td, *J* = 7.6, 1.2 Hz, 1H), 7.44 (dd, *J* = 8.0, 1.6 Hz, 1H), 7.52 (br s, 1H), 7.57 (dd, *J* = 8.0, 1.2 Hz, 1H), 7.60 (br s, 1H), 8.92 (br s, 1H); ^{13}C NMR (100 MHz, CD_3OD): δ 29.8, 35.8, 39.2, 54.6, 70.8, 77.7, 110.0, 120.7, 124.9, 125.1, 128.5, 129.2, 129.5, 130.4, 131.0, 132.8, 134.2, 137.8, 138.3, 141.3; HRMS (ESI) $[M-Cl]^+$

Calcd for $C_{22}H_{23}BrClN_2O_2S$: 493.0352. Found: 493.0343. Anal. Calcd for $C_{22}H_{23}BrCl_2N_2O_2S$: C, 49.83; H, 4.37; N, 5.28. Found: C, 49.66; H, 4.47; N, 5.08.

4.5. Representative procedure for the displacement of the *p*-toluenesulfonyloxy group in compound 4 using phenol-containing nucleophiles

4.5.1. (2*R*,4*S*)-2-[2-(4-Chlorophenyl)ethyl]-2-[(1*H*-imidazol-1-yl)methyl]-4-(phenoxymethyl)-1,3-dioxolane hydrochloride (23)

Under a N_2 atmosphere, a mixture of (2*R*,4*S*)-2-[2-(4-chlorophenyl)ethyl]-2-[(1*H*-imidazol-1-yl)methyl]-4-[(*p*-toluenesulfonyloxy)methyl]-1,3-dioxolane (**4**)[11] (100 mg, 0.21 mmol), phenol (79 mg, 0.84 mmol, 4 equiv), and cesium carbonate (205 mg, 0.63 mmol, 6 equiv) in *N*,*N*-dimethylformamide (3 mL) was heated at 90 °C with stirring for 8 h. The mixture was diluted with H_2O, extracted with EtOAc (3×), and the combined organic extracts were washed sequentially with a saturated aqueous solution of Na_2CO_3, and brine, and then dried ($MgSO_4$). The solution was concentrated, and the residue was purified by flash chromatography on silica gel (EtOAc) to give the free base (60 mg, 0.15 mmol) as an oil (R_f = 0.38, EtOAc). To a solution of this oil in warm 2-propanol (2 mL) was added a solution of 37% aqueous HCl (34 mg, 0.35 mmol, 2.3 equiv) in 2-propanol (2 mL). The mixture was concentrated and dried under high vacuum. The residue was dissolved in 2-propanol (0.5 mL), the solution cooled in the freezer, and then a few drops of Et_2O were added and the product allowed to crystallize overnight. The solid was removed by filtration and washed with Et_2O. High-vacuum drying gave **23** (79 mg, 0.18 mmol, 86%) as a white solid: mp 139–140 °C; $[\alpha]_D^{23}$ −18.3 (*c* 0.5 in CD_3OD); ^1H NMR (400 MHz, CD_3OD): δ 2.04 (t, *J* = 8.4 Hz, 2H), 2.70–2.88 (m, 2H), 3.96 (t, *J* = 7.6 Hz, 1H), 4.00–4.08 (m, 2H), 4.09–4.17 (m, 2H), 4.52 (s, 2H), 6.88–6.91 (m, 2H), 6.94 (t, *J* = 7.4 Hz, 1H), 7.15 (d, *J* = 8.4 Hz, 2H), 7.20–7.31 (m, 4H), 7.59 (br s, 1H), 7.67 (br s, 1H), 9.00 (br s, 1H); ^{13}C NMR (100 MHz, CD_3OD): δ 29.8, 39.0, 54.6, 68.2, 68.3, 77.5, 110.0, 115.6, 120.6, 122.3, 125.1, 129.5, 130.6, 131.0, 132.8, 137.8, 141.5, 160.0; HRMS (ESI) $[M-Cl]^+$ Calcd for $C_{22}H_{24}ClN_2O_3$: 399.1475. Found: 399.1466. Anal. Calcd for $C_{22}H_{24}Cl_2N_2O_3$: C, 60.70; H, 5.56; N, 6.43. Found: C, 60.90; H, 5.51; N, 6.39.

4.6. Characterization of the new compounds synthesized following the representative procedure described above for compound 23, as outlined in Scheme 1

4.6.1. (2*R*,4*S*)-4-[(4-Aminophenoxy)methyl]-2-[2-(4-chlorophenyl)ethyl]-2-[(1*H*-imidazol-1-yl)methyl]-1,3-dioxolane dihydrochloride (20)

Hygroscopic white solid in 54% yield from **4**[11]: R_f = 0.17 (free base, EtOAc); $[\alpha]_D^{22}$ −12.9 (*c* 0.9 in CD_3OD); ^1H NMR (400 MHz, CD_3OD): δ 2.04 (t, *J* = 8.4 Hz, 2H), 2.70–2.88 (m, 2H), 3.97 (t, *J* = 6.8 Hz, 1H), 4.03–4.20 (m, 4H), 4.53 (s, 2H), 7.06 (d, *J* = 8.8 Hz, 2H), 7.16 (d, *J* = 8.0 Hz, 2H), 7.24 (d, *J* = 8.4 Hz, 2H), 7.33 (d, *J* = 8.8 Hz, 2H), 7.60 (br s, 1H), 7.67 (br s, 1H), 9.00 (br s, 1H); ^{13}C NMR (100 MHz, CD_3OD): δ 29.8, 38.9, 54.5, 68.1, 68.9, 77.3, 110.1, 117.0, 120.6, 125.1, 125.2, 125.3, 129.5, 131.0, 132.8, 137.9, 141.5, 160.2; HRMS (ESI) $[M-H-2Cl]^+$ Calcd for $C_{22}H_{25}ClN_3O_3$: 414.1584. Found: 414.1565. Anal. Calcd for $C_{22}H_{26}Cl_3N_3O_3$: C, 54.28; H, 5.38; N, 8.63. Found: C, 54.48; H, 5.60; N, 8.59.

4.6.2. (2*R*,4*S*)-2-[2-(4-Chlorophenyl)ethyl]-4-[(4-hydroxyphenoxy)methyl]-2-[(1*H*-imidazol-1-yl)methyl]-1,3-dioxolane hydrochloride (21)

White solid in 33% yield from **4**[11]: mp 128–130 °C; R_f = 0.17 (EtOAc); $[\alpha]_D^{22}$ −14.4 (*c* 0.8 in CD_3OD); ^1H NMR (400 MHz, CD_3OD): δ 2.03 (t, *J* = 8.6 Hz, 2H), 2.70–2.87 (m, 2H), 3.88–4.12 (m, 5H), 4.51 (s, 2H), 6.70 (d, *J* = 8.8 Hz, 2H), 6.75 (d, *J* = 9.2 Hz, 2H), 7.15 (d, *J* = 8.4 Hz, 2H), 7.24 (d, *J* = 8.4 Hz, 2H), 7.58 (∼t, *J* = 1.6 Hz, 1H), 7.65 (∼t, *J* = 1.6 Hz, 1H), 8.97 (br s, 1H); ^{13}C NMR (100 MHz, CD_3OD): δ 29.8, 39.1, 54.7, 68.3, 69.4, 77.7, 110.0, 116.8, 116.9, 120.6, 125.2, 129.5, 131.0, 132.8, 137.8, 141.5, 152.9, 153.3; HRMS (ESI) $[M-Cl]^+$ Calcd for $C_{22}H_{24}ClN_2O_4$: 415.1425. Found: 415.1407. Anal. Calcd for $C_{22}H_{24}Cl_2N_2O_4$: C, 58.54; H, 5.36; N, 6.21. Found: C, 58.50; H, 5.47; N, 6.13.

4.6.3. (2*R*,4*S*)-4-[{(4-Adamantan-1-yl)phenoxy}methyl]-2-[2-(4-chlorophenyl)ethyl]-2-[(1*H*-imidazol-1-yl)methyl]-1,3-dioxolane hydrochloride (22)

White solid in 72% yield from **4**[11]: mp 132–134 °C; R_f = 0.22 (free base, EtOAc); $[\alpha]_D^{22}$ −11.8 (*c* 0.6 in CD_3OD); ^1H NMR (400 MHz, CD_3OD): δ 1.74–1.91 (m, 13H), 2.02 (t, *J* = 8.6 Hz, 2H), 2.04–2.10 (m, 2H), 2.70–2.84 (m, 2H), 3.94–4.05 (m, 3H), 4.06–4.15 (m, 2H), 4.51 (s, 2H), 6.84 (d, *J* = 9.2 Hz, 2H), 7.13 (d, *J* = 8.4 Hz, 2H), 7.23 (d, *J* = 8.4 Hz, 2H), 7.26 (d, *J* = 8.8 Hz, 2H), 7.59 (br s, 1H), 7.66 (br s, 1H), 8.98 (br s, 1H); ^{13}C NMR (100 MHz, CD_3OD): δ 29.8, 30.5, 36.7, 37.9, 39.0, 44.6, 54.6, 68.2, 68.5, 77.7, 110.0, 115.2, 120.6, 125.1, 126.9, 129.5, 131.0, 132.8, 137.8, 141.5, 145.6, 157.8; HRMS (ESI) $[M-Cl]^+$ Calcd for $C_{32}H_{38}ClN_2O_3$: 533.2571. Found: 533.2581. Anal. Calcd for $C_{32}H_{38}Cl_2N_2O_3$: C, 67.48; H, 6.72; N, 4.92. Found: C, 66.85; H, 7.33; N, 4.37.

4.6.4. (2*R*,4*S*)-4-[(4-Bromophenoxy)methyl]-2-[2-(4-chlorophenyl)ethyl]-2-[(1*H*-imidazol-1-yl)methyl]-1,3-dioxolane hydrochloride (24)

Hygroscopic white solid in 76% yield from **4**[11]: mp 55–57 °C in air; R_f = 0.22 (free base, EtOAc); $[\alpha]_D^{25}$ −16.3 (*c* 0.6 in CD_3OD); ^1H NMR (400 MHz, CD_3OD): δ 2.02 (t, *J* = 8.4 Hz, 2H), 2.69–2.84 (m, 2H), 3.88–4.06 (m, 3H), 4.11 (t, *J* = 6.8 Hz, 2H), 4.51 (s, 2H), 6.85 (d, *J* = 9.2 Hz, 2H), 7.14 (d, *J* = 8.8 Hz, 2H), 7.24 (d, *J* = 8.8 Hz, 2H), 7.39 (d, *J* = 8.8 Hz, 2H), 7.59 (br s, 1H), 7.66 (br s, 1H), 8.98 (br s, 1H); ^{13}C NMR (100 MHz, CD_3OD): δ 29.8, 38.9, 54.6, 68.1, 68.7, 77.4, 110.1, 114.3, 117.6, 120.7, 125.1, 129.6, 131.0, 132.9, 133.5, 137.9, 141.4, 159.2; HRMS (ESI) $[M-Cl]^+$ Calcd for $C_{22}H_{23}BrClN_2O_3$: 477.0581. Found: 477.0557. Anal. Calcd for $C_{22}H_{23}BrCl_2N_2O_3$: C, 51.38; H, 4.51; N, 5.45. Found: C, 51.44; H, 4.37; N, 5.25.

4.6.5. (2*R*,4*S*)-2-[2-(4-Chlorophenyl)ethyl]-4-[(4-fluorophenoxy)methyl]-2-[(1*H*-imidazol-1-yl)methyl]-1,3-dioxolane hydrochloride (25)

Hygroscopic white solid in 86% yield from **4**[11]: mp 50–52 °C in air; R_f = 0.23 (free base, EtOAc); $[\alpha]_D^{24}$ −20.8 (*c* 0.5 in CD_3OD); ^1H NMR (400 MHz, CD_3OD): δ 2.04 (t, *J* = 8.4 Hz, 2H), 2.71–2.87 (m, 2H), 3.88–4.15 (m, 5H), 4.52 (s, 2H), 6.86–6.93 (m, 2H), 7.00 (∼t, *J* = 8.8 Hz, 2H), 7.16 (d, *J* = 8.4 Hz, 2H), 7.25 (d, *J* = 8.4 Hz, 2H), 7.59 (br s, 1H), 7.66 (br s, 1H), 8.98 (br s, 1H); ^{13}C NMR (100 MHz, CD_3OD): δ 29.8, 39.0, 54.6, 68.2, 69.2, 77.5, 110.1, 116.8 (d, $^2J_{C-F}$ = 11.9 Hz), 116.9 (d, $^3J_{C-F}$ = 3.5 Hz), 120.6, 125.1, 129.5, 131.0, 132.8, 137.8, 141.5, 156.2 (d, $^4J_{C-F}$ = 1.8 Hz), 158.9 (d, $^1J_{C-F}$ = 237.5 Hz); ^{19}F NMR (376 MHz, CD_3OD): δ −126.6; HRMS (ESI) $[M-Cl]^+$ Calcd for $C_{22}H_{23}ClFN_2O_3$: 417.1381. Found: 417.1366. Anal. Calcd for $C_{22}H_{23}Cl_2FN_2O_3$: C, 58.29; H, 5.11; N, 6.18. Found: C, 58.27; H, 5.16; N, 6.00.

4.6.6. (2*R*,4*S*)-4-[(Biphenyl-4-yloxy)methyl]-2-[2-(4-chlorophenyl)ethyl]-2-[(1*H*-imidazol-1-yl)methyl]-1,3-dioxolane hydrochloride (26)

White solid in 43% yield from **4**[11]: mp 162–163 °C; R_f = 0.12 (EtOAc); $[\alpha]_D^{23}$ −23.5 (*c* 0.6 in CD_3OD); ^1H NMR (400 MHz, CD_3OD): δ 2.04 (t, *J* = 8.4 Hz, 2H), 2.70–2.90 (m, 2H), 3.98 (t, *J* = 7.4 Hz, 1H), 4.02–4.10 (m, 2H), 4.10–4.15 (m, 1H), 4.16–4.22 (m, 1H), 4.52 (s, 2H), 6.99 (d, *J* = 8.8 Hz, 2H), 7.14 (d, *J* = 8.4 Hz, 2H), 7.23 (d,

J = 8.4 Hz, 2H), 7.28 (t, J = 7.4 Hz, 1H), 7.39 (t, J = 7.8 Hz, 2H), 7.50–7.56 (m, 4H), 7.60 (br s, 1H), 7.67 (br s, 1H), 9.00 (br s, 1H); ^{13}C NMR (100 MHz, CD_3OD): δ 29.8, 39.0, 54.6, 68.2, 68.5, 77.6, 110.1, 116.0, 120.6, 125.1, 127.6, 127.8, 129.1, 129.5, 129.8, 131.0, 132.8, 135.6, 137.8, 141.5, 141.9, 159.6; HRMS (ESI) $[M-Cl]^+$ Calcd for $C_{28}H_{28}ClN_2O_3$: 475.1788. Found: 475.1779. Anal. Calcd for $C_{28}H_{28}Cl_2N_2O_3$: C, 65.76; H, 5.52; N, 5.48. Found: C, 65.58; H, 5.42; N, 5.37.

4.6.7. (2*R*,4*S*)-2-[2-(4-Chlorophenyl)ethyl]-2-[(1*H*-imidazol-1-yl)methyl]-4-[(4-methoxyphenoxy)methyl]-1,3-dioxolane hydrochloride (27)

White solid in 81% yield from **4**[11]: mp 128–129 °C; R_f = 0.29 (free base, EtOAc); $[\alpha]_D^{23}$ −16.8 (c 0.5 in CD_3OD); ^{1}H NMR (400 MHz, CD_3OD): δ 2.03 (t, J = 8.4 Hz, 2H), 2.71–2.86 (m, 2H), 3.73 (s, 3H), 3.90–4.04 (m, 3H), 4.04–4.13 (m, 2H), 4.51 (s, 2H), 6.83 (br s, 4H), 7.15 (d, J = 8.4 Hz, 2H), 7.24 (d, J = 8.4 Hz, 2H), 7.59 (br s, 1H), 7.66 (br s, 1H), 8.98 (br s, 1H); ^{13}C NMR (100 MHz, CD_3OD): δ 29.8, 39.0, 54.6, 56.1, 68.3, 69.2, 77.6, 110.0, 115.7, 116.6, 120.6, 125.1, 129.5, 131.0, 132.8, 137.8, 141.5, 154.1, 155.8; HRMS (ESI) $[M-Cl]^+$ Calcd for $C_{23}H_{26}ClN_2O_4$: 429.1581. Found: 429.1567. Anal. Calcd for $C_{23}H_{26}Cl_2N_2O_4$: C, 59.36; H, 5.63; N, 6.02. Found: C, 59.50; H, 5.56; N, 6.03.

4.6.8. (2*R*,4*S*)-2-[2-(4-Chlorophenyl)ethyl]-2-[(1*H*-imidazol-1-yl)methyl]-4-[(4-iodophenoxy)methyl]-1,3-dioxolane hydrochloride (28)

White solid in 67% yield from **4**[11]: mp 113–114 °C; R_f = 0.29 (free base, EtOAc); $[\alpha]_D^{24}$ −12.7 (c 0.7 in CD_3OD); ^{1}H NMR (400 MHz, CD_3OD): δ 2.01 (t, J = 8.4 Hz, 2H), 2.69–2.84 (m, 2H), 3.90–3.97 (m, 1H), 3.98–4.07 (m, 2H), 4.08–4.16 (m, 2H), 4.51 (s, 2H), 6.73 (d, J = 8.8 Hz, 2H), 7.13 (d, J = 8.4 Hz, 2H), 7.24 (d, J = 8.4 Hz, 2H), 7.56 (d, J = 8.8 Hz, 2H), 7.58 (br s, 1H), 7.65 (br s, 1H), 8.97 (br s, 1H); ^{13}C NMR (100 MHz, CD_3OD): δ 29.8, 38.9, 54.6, 68.1, 68.5, 77.4, 110.1, 118.1, 120.7, 125.1, 129.5, 131.0, 132.8, 137.9, 139.5 (2C), 141.4, 160.0; HRMS (ESI) $[M-Cl]^+$ Calcd for $C_{22}H_{23}ClIN_2O_3$: 525.0442. Found: 525.0440. Anal. Calcd for $C_{22}H_{23}Cl_2IN_2O_3$: C, 47.08; H, 4.13; N, 4.99. Found: C, 47.21; H, 4.33; N, 4.95.

4.6.9. (2*R*,4*S*)-2-[2-(4-Chlorophenyl)ethyl]-4-[(4-cyanophenoxy)methyl]-2-[(1*H*-imidazol-1-yl)methyl]-1,3-dioxolane hydrochloride (29)

Hygroscopic white solid in 100% yield from **4**[11]: R_f = 0.26 (free base, EtOAc); $[\alpha]_D^{21}$ −15.3 (c 0.5 in CD_3OD); ^{1}H NMR (400 MHz, CD_3OD): δ 2.03 (dd, J = 9.2, 7.6 Hz, 2H), 2.70–2.85 (m, 2H), 3.96 (t, J = 7.8 Hz, 1H), 4.04–4.17 (m, 3H), 4.23 (dd, J = 10.2, 3.0 Hz, 1H), 4.52 (s, 2H), 7.06 (d, J = 8.8 Hz, 2H), 7.15 (d, J = 8.4 Hz, 2H), 7.24 (d, J = 8.4 Hz, 2H), 7.60 (br s, 1H), 7.63–7.68 (m, 3H), 8.99 (br s, 1H); ^{13}C NMR (100 MHz, CD_3OD): δ 29.7, 38.8, 54.5, 68.0, 68.7, 77.2, 105.4, 110.2, 116.6, 119.9, 120.7, 125.1, 129.6, 131.0, 132.9, 135.3, 137.9, 141.4, 163.4; HRMS (ESI) $[M-Cl]^+$ Calcd for $C_{23}H_{23}ClN_3O_3$: 424.1428. Found: 424.1409. Anal. Calcd for $C_{23}H_{23}Cl_2N_3O_3$: C, 60.01; H, 5.04; N, 9.13. Found: C, 59.84; H, 5.09; N, 8.96.

4.7. Procedures for the displacement of the *p*-toluenesulfonyloxy group in compound 4 using various nucleophiles as outlined in Scheme 2

4.7.1. (2*R*,4*R*)-2-[2-(4-Chlorophenyl)ethyl]-4-(hydroxymethyl)-2-[(1*H*-imidazol-1-yl)methyl]-1,3-dioxolane hydrochloride (30)

To a mixture of (2*R*,4*S*)-2-[2-(4-chlorophenyl)ethyl]-2-[(1*H*-imidazol-1-yl)methyl]-4-[(*p*-toluenesulfonyloxy)methyl]-1,3-dioxolane (**4**)[11] (91 mg, 0.19 mmol) in *N*,*N*-dimethylformamide (6 mL) was added KOH (210 mg, 3.74 mmol, 20 equiv) and a small amount of LiOH. The mixture heated at 120 °C with stirring for 9 h. The reaction mixture was cooled to room temperature, diluted with H_2O, and extracted with EtOAc (2×), and the combined organic extracts were washed sequentially with a saturated aqueous solution of Na_2CO_3, and water, and then dried ($MgSO_4$). The solution was concentrated, and the residue was purified by preparative thin-layer chromatography on silica gel (load with MeOH, elute with EtOAc) to give the free base (40 mg, 0.12 mmol) as an oil ($R_f \sim$ 0.2–0.3, EtOAc). To a solution of the free base in warm 2-propanol (2 mL) was added a solution of 37% aqueous HCl (20 mg, 0.20 mmol, 1.7 equiv) in 2-propanol (2 mL). The mixture was concentrated, dried under high vacuum, and washed with Et_2O. High-vacuum drying gave **30** (30 mg, 0.08 mmol, 42%) as a white solid: mp 159–160 °C; R_f = 0.07 (EtOAc); $[\alpha]_D^{22}$ −6.3 (c 0.6 in CD_3OD); ^{1}H NMR (400 MHz, CD_3OD): δ 1.98 (t, J = 8.6 Hz, 2H), 2.70–2.88 (m, 2H), 3.53–3.67 (m, 2H), 3.68–3.79 (m, 2H), 4.01 (t, J = 6.6 Hz, 1H), 4.47 (s, 2H), 7.20 (d, J = 8.0 Hz, 2H), 7.27 (d, J = 8.4 Hz, 2H), 7.57 (br s, 1H), 7.63 (br s, 1H), 8.94 (br s, 1H); ^{13}C NMR (100 MHz, CD_3OD): δ 29.7, 39.2, 54.7, 62.8, 68.4, 79.6, 109.7, 120.7, 125.1, 129.5, 131.0, 132.8, 137.9, 141.5; HRMS (ESI) $[M-Cl]^+$ Calcd for $C_{16}H_{20}ClN_2O_3$: 323.1162. Found: 323.1170.

4.7.2. (2*R*,4*S*)-2-[2-(4-Chlorophenyl)ethyl]-2-[(1*H*-imidazol-1-yl)methyl]-4-[(methylthio)methyl]-1,3-dioxolane hydrochloride (31)

A mixture of (2*R*,4*S*)-2-[2-(4-chlorophenyl)ethyl]-2-[(1*H*-imidazol-1-yl)methyl]-4-[(*p*-toluenesulfonyloxy)methyl]-1,3-dioxolane (**4**)[11] (135 mg, 0.28 mmol), sodium thiomethoxide (51 mg, 0.73 mmol, 2.6 equiv), and cesium carbonate (91 mg, 0.28 mmol, 2 equiv) in acetone (6 mL) was heated at reflux temperature with stirring for 6 h. The reaction mixture was concentrated, and hot EtOAc was added. The solids were removed by filtration and washed with hot EtOAc and then with acetone. The organic filtrate was concentrated, and the residue was purified by flash chromatography on silica gel (EtOAc) to give the free base (~110 mg) as a golden oil (R_f = 0.28, EtOAc). To a solution of the free base in warm 2-propanol (2 mL) was added a solution of 37% aqueous HCl (35 mg, 0.36 mmol, 1.3 equiv) in 2-propanol (2 mL). The mixture was concentrated and dried under high vacuum. The residue was dissolved in 2-propanol (1 mL), the solution cooled in the freezer, and then a few drops of Et_2O were added and the product allowed to crystallize overnight. The solid was removed by filtration and washed with Et_2O. High-vacuum drying gave **31** (98 mg, 0.25 mmol, 89%) as a white solid: mp 142–143 °C; R_f = 0.20 (EtOAc); $[\alpha]_D^{22}$ −11.9 (c 1.0 in CD_3OD); ^{1}H NMR (400 MHz, CD_3OD): δ 2.00 (dd, J = 9.4, 7.8 Hz, 2H), 2.65 (dd, J = 13.6, 6.0 Hz, 1H), 2.70–2.85 (m, 3H), 3.71 (t, J = 8.0 Hz, 1H), 3.75–3.82 (m, 1H), 4.09 (dd, J = 8.0, 5.6 Hz, 1H), 4.48 (s, 2H), 4.86 (s, 3H), 7.21 (d, J = 8.8 Hz, 2H), 7.27 (d, J = 8.4 Hz, 2H), 7.59 (br s, 1H), 7.64 (br s, 1H), 8.96 (br s, 1H); ^{13}C NMR (100 MHz, CD_3OD): δ 16.4, 29.9, 37.0, 39.2, 54.7, 71.1, 78.8, 109.8, 120.6, 125.1, 129.6, 131.0, 132.9, 137.8, 141.4; HRMS (ESI) $[M-Cl]^+$ Calcd for $C_{17}H_{22}ClN_2O_2S$: 353.1090. Found: 353.1086. Anal. Calcd for $C_{17}H_{22}Cl_2N_2O_2S$: C, 52.44; H, 5.70; N, 7.20. Found: C, 52.51; H, 5.51; N, 7.12.

4.7.3. (2*R*,4*S*)-2-[2-(4-Chlorophenyl)ethyl]-4-(fluoromethyl)-2-[(1*H*-imidazol-1-yl)methyl]-1,3-dioxolane hydrochloride (32)

To a sample of (2*R*,4*S*)-2-[2-(4-chlorophenyl)ethyl]-2-[(1*H*-imidazol-1-yl)methyl]-4-[(*p*-toluenesulfonyloxy)methyl]-1,3-dioxolane (**4**)[11] (120 mg, 0.25 mmol) was added a 1 M solution of tetra-*n*-butylammonium fluoride in THF (5 mL, 5.0 mmol, 20 equiv) and the mixture was heated at reflux temperature with stirring for 18.5 h. The reaction mixture was cooled to room temperature, diluted with H_2O, and extracted with EtOAc (3×), and the combined organic extracts were washed sequentially with a saturated aqueous solution of Na_2CO_3, and water, and then dried ($MgSO_4$). The

solution was concentrated and the residue purified by flash column chromatography on silica gel (EtOAc) to give the free base (70 mg, 0.22 mmol) as a golden oil (R_f = 0.21, EtOAc). To a solution of the free base in warm 2-propanol (2 mL) was added a solution of 37% aqueous HCl (25 mg, 0.25 mmol, 1.1 equiv) in 2-propanol (2 mL). The mixture was concentrated and dried under high vacuum. The residue was dissolved in 2-propanol (1 mL), the solution cooled in the freezer, and then a few drops of Et_2O were added and the product allowed to crystallize overnight. The solid was removed by filtration and washed with Et_2O. High-vacuum drying gave **32** (72 mg, 0.20 mmol, 80%) as a white solid: mp 128–129 °C; $[\alpha]_D^{22}$ −6.0 (*c* 1.0 in CD_3OD); ^1H NMR (400 MHz, CD_3OD): δ 1.99 (t, *J* = 8.6 Hz, 2H), 2.69–2.84 (m, 2H), 3.86 (t, *J* = 7.8 Hz, 1H), 3.90–4.00 (m, 1H), 4.06 (t, *J* = 6.6 Hz, 1H), 4.35 (∼dd, *J* = 10.8, 4.0 Hz, 0.5H), 4.44–4.49 (m, 1H), 4.51 (s, 2H), 4.61 (∼dd, *J* = 10.6, 2.6 Hz, 0.5H), 7.20 (d, *J* = 8.4 Hz, 2H), 7.27 (d, *J* = 8.4 Hz, 2H), 7.59 (br s, 1H), 7.64 (br s, 1H), 8.98 (br s, 1H); ^{13}C NMR (100 MHz, CD_3OD): δ 29.7, 38.9, 54.4, 66.7 (d, $^3J_{C-F}$ = 7.6 Hz), 77.7 (d, $^2J_{C-F}$ = 19.5 Hz), 82.8 (d, $^1J_{C-F}$ = 172.7 Hz), 110.1, 120.6, 125.1, 129.6, 131.0, 132.8, 137.8, 141.4; ^{19}F–$^1H_{dec}$ (376 MHz, CD_3OD): δ -234.1; HRMS (ESI) $[M-Cl]^+$ Calcd for $C_{16}H_{19}ClFN_2O_2$: 325.1119. Found: 325.1124. Anal. Calcd for $C_{16}H_{19}Cl_2FN_2O_2$: C, 53.20; H, 5.30; N, 7.75. Found: C, 53.21; H, 5.23; N, 7.59.

4.7.4. (2*R*,4*R*)-2-[2-(4-Chlorophenyl)ethyl]-2-[(1*H*-imidazol-1-yl)methyl]-4-[(1*H*-imidazol-1-yl)methyl]-1,3-dioxolane dihydrochloride dihydrate (33)

To a mixture of (2*R*,4*S*)-2-[2-(4-chlorophenyl)ethyl]-2-[(1*H*-imidazol-1-yl)methyl]-4-[(*p*-toluenesulfonyloxy)methyl]-1,3-dioxolane (**4**)[11] (105 mg, 0.22 mmol) in *N*,*N*-dimethylformamide (2.5 mL) was added imidazole (120 mg, 1.76 mmol, 8 equiv). The mixture heated at 110 °C with stirring for 30 h. The reaction mixture was cooled to room temperature, diluted with H_2O, and extracted with $CHCl_3$ (3×), and the combined organic extracts were washed with water, and then dried (Na_2SO_4). The solution was concentrated, and the residue was purified by flash column chromatography on silica gel (load with hot EtOAc, elute with acetone) to give the free base (80 mg, 0.21 mmol) as an oil (R_f ∼ 0.16, EtOAc). To a solution of the free base in warm 2-propanol (1 mL) was added a solution of 37% aqueous HCl (56 mg, 0.57 mmol, 2.7 equiv) in 2-propanol (1 mL). The mixture was concentrated, CH_2Cl_2 (5 mL) added, and the mixture concentrated again. High-vacuum drying gave **33** (90 mg, 0.19 mmol, 86%) as a hygroscopic white solid in the dihydrochloride dihydrate form: mp 145 °C (fully melted); $[\alpha]_D^{22}$ +6.8 (*c* 0.9 in CD_3OD); ^1H NMR (400 MHz, CD_3OD): δ 1.90–2.06 (m, 2H), 2.63–2.82 (m, 2H), 3.79 (t, *J* = 8.6 Hz, 1H), 4.07–4.15 (m, 1H), 4.25 (dd, *J* = 8.6, 6.6 Hz, 1H), 4.39 (dd, *J* = 14.4, 7.2 Hz, 1H), 4.54 (s, 2H), 4.60 (dd, *J* = 14.4, 2.8 Hz, 1H), 7.22 (d, *J* = 8.4 Hz, 2H), 7.28 (d, *J* = 8.4 Hz, 2H), 7.56–7.72 (m, 4H), 8.98 (s, 1H), 9.02 (s, 1H); ^{13}C NMR (100 MHz, CD_3OD): δ 29.6, 38.6, 51.6, 54.2, 68.5, 76.9, 110.8, 120.8, 121.2, 124.2, 125.0, 129.6, 131.0, 133.0, 137.3, 137.8, 141.1; HRMS (ESI) $[M-5H-2Cl-2O]^+$ Calcd for $C_{19}H_{22}ClN_4O_2$: 373.1431. Found: 373.1429. Anal. Calcd for $C_{19}H_{27}Cl_3N_4O_4$: C, 47.36; H, 5.65; N, 11.63. Found: C, 47.83; H, 5.51; N, 11.41.

4.7.5. (2*R*,4*S*)-4-(Chloromethyl)-2-[2-(4-chlorophenyl)ethyl]-2-[(1*H*-imidazol-1-yl)methyl]-1,3-dioxolane hydrochloride monohydrate (34)

To a mixture of (2*R*,4*S*)-2-[2-(4-chlorophenyl)ethyl]-2-[(1*H*-imidazol-1-yl)methyl]-4-[(*p*-toluenesulfonyloxy)methyl]-1,3-dioxolane (**4**)[11] (108 mg, 0.23 mmol) in *N*,*N*-dimethylformamide (3 mL) was added lithium chloride (192 mg, 4.53 mmol, 19.7 equiv). The mixture was heated at 110 °C with stirring for 1 h. The reaction mixture was cooled to room temperature, diluted with H_2O, and extracted with EtOAc (3×), and the combined organic extracts were washed sequentially with a saturated aqueous solution of Na_2CO_3, and H_2O, and then dried (Na_2SO_4). The solution was concentrated and dried under high vacuum to give the clean free base (90 mg) as an oil (R_f = 0.24, EtOAc). To a solution of the free base in warm 2-propanol (2 mL) was added a solution of 37% aqueous HCl (40 mg, 0.41 mmol, 2.7 equiv) in 2-propanol (2 mL). The mixture was concentrated and dried under high vacuum. The residue was dissolved in the least amount of hot 2-propanol, the solution cooled at room temperature, and then at −25 °C in a freezer prior to the gradual addition of diethyl ether to complete the precipitation of the hydrochloride. The product was collected by filtration and washed with diethyl ether. High-vacuum drying gave **34** (74 mg, 0.19 mmol, 83%) as a white solid in the hydrochloride monohydrate form: mp 118–119 °C; $[\alpha]_D^{24}$ −16.2 (*c* 0.4 in CD_3OD); ^1H NMR (400 MHz, CD_3OD): δ 1.96–2.05 (m, 2H), 2.72–2.86 (m, 2H), 3.63–3.73 (m, 2H), 3.86 (t, *J* = 8.0 Hz, 1H), 3.91–3.98 (m, 1H), 4.09 (dd, *J* = 8.4, 6.0 Hz, 1H), 4.44–4.55 (m, 2H), 7.21 (d, *J* = 8.8 Hz, 2H), 7.27 (d, *J* = 8.4 Hz, 2H), 7.59 (s, 1H), 7.65 (s, 1H), 8.97 (s, 1H); ^{13}C NMR (100 MHz, CD_3OD): δ 29.8, 39.0, 44.7, 54.4, 69.3, 78.2, 110.2, 120.7, 125.1, 129.6, 131.0, 132.9, 137.8, 141.3; HRMS (ESI) $[M-2H-Cl-O]^+$ Calcd for $C_{16}H_{19}Cl_2N_2O_2$: 341.0824. Found: 341.0817. Anal. Calcd for $C_{16}H_{21}Cl_3N_2O_3$: C, 48.56; H, 5.35; N, 7.08. Found: C, 49.88; H, 5.16; N, 6.30.

4.7.6. (2*R*,4*R*)-4-(Azidomethyl)-2-[2-(4-chlorophenyl)ethyl]-2-[(1*H*-imidazol-1-yl)methyl]-1,3-dioxolane (35)

To a mixture of (2*R*,4*S*)-2-[2-(4-chlorophenyl)ethyl]-2-[(1*H*-imidazol-1-yl)methyl]-4-[(*p*-toluenesulfonyloxy)methyl]-1,3-dioxolane (**4**)[11] (201 mg, 0.42 mmol) in *N*,*N*-dimethylformamide (3 mL) was added sodium azide (546 mg, 8.40 mmol, 20 equiv). The mixture was heated at 110 °C with stirring for 2 h. The reaction mixture was cooled to room temperature, diluted with H_2O, and extracted with EtOAc (3×), and the combined organic extracts were washed sequentially with a saturated aqueous solution of Na_2CO_3, and H_2O, and then dried (Na_2SO_4). The solution was concentrated and the golden oily residue purified by flash column chromatography on silica gel (EtOAc) to give the free base as an oil (R_f = 0.29, EtOAc). High-vacuum drying gave **35** (121 mg, 0.35 mmol, 83%) as a colorless oil: $[\alpha]_D^{24}$ +6.6 (*c* 0.7 in $CDCl_3$); ^1H NMR (400 MHz, $CDCl_3$): δ 1.90–2.05 (m, 2H), 2.66–2.81 (m, 2H), 3.20 (dd, *J* = 13.2, 5.2 Hz, 1H), 3.39 (dd, *J* = 13.2, 4.0 Hz, 1H), 3.44–3.51 (m, 1H), 3.64 (t, *J* = 8.0 Hz, 1H), 3.78 (dd, *J* = 8.0, 6.4 Hz, 1H), 4.02 (s, 2H), 6.98 (br s, 1H), 7.05 (br s, 1H), 7.12 (d, *J* = 8.4 Hz, 2H), 7.25 (d, *J* = 8.4 Hz, 2H), 7.49 (br s, 1H); ^{13}C NMR (100 MHz, $CDCl_3$): δ 29.0, 38.7, 51.8, 53.0, 67.9, 76.1, 109.9, 120.9, 128.8, 129.3, 129.8, 132.1, 138.7, 139.6; HRMS (EI) $[M+H]^+$ Calcd for $C_{16}H_{19}ClN_5O_2$: 348.1227. Found: 348.1234. Anal. Calcd for $C_{16}H_{18}ClN_5O_2$: C, 55.25; H, 5.22; N, 20.14. Found: C, 55.10; H, 5.18; N, 19.88.

4.7.7. (2*R*,4*R*)-4-(Aminomethyl)-2-[(1*H*-imidazol-1-yl)methyl]-2-[(2-phenyl)ethyl]-1,3-dioxolane dihydrochloride (36)

To a sample of 10% Pd/C catalyst (25 mg) under an atmosphere of N_2, was carefully added MeOH (5 mL). To this suspension was then added the azide **35** (87 mg, 0.25 mmol) along with ammonium formate (100 mg, 1.59 mmol, 6.4 equiv). The mixture was heated to reflux temperature for 3 h, and then filtered through Celite. The filter cake was washed with MeOH, and the filtrate and washings were combined and concentrated. The residue was diluted with a saturated aqueous solution of Na_2CO_3, and extracted with EtOAc (2×), and the combined organic extracts were washed sequentially with a saturated aqueous solution of Na_2CO_3, and brine, and then dried ($MgSO_4$). The solution was concentrated and dried under high vacuum. To a solution of the free base (∼30 mg, 0.10 mmol) in warm EtOH (2 mL) was added a solution of 37% aqueous HCl (40 mg, 0.41 mmol, 4.6 equiv) in EtOH (2 mL);

the mixture was concentrated. High-vacuum drying gave **36** (40 mg, 0.10 mmol, 40%) as a white hygroscopic solid: $[\alpha]_D^{19}$ +3.7 (*c* 1.7 in CD_3OD); ^1H NMR (400 MHz, CD_3OD): δ 2.00–2.10 (m, 2H), 2.76–2.86 (m, 2H), 3.14 (dd, *J* = 13.4, 9.8 Hz, 1H), 3.26 (dd, *J* = 13.2, 2.0 Hz, 1H), 3.78 (t, *J* = 8.0 Hz, 1H), 4.14–4.24 (m, 1H), 4.25 (dd, *J* = 8.4, 6.4 Hz, 1H), 4.56 (s, 2H), 7.15–7.34 (m, 5H), 7.61 (s, 1H), 7.69 (s, 1H), 9.06 (s, 1H); ^{13}C NMR (100 MHz, CD_3OD): δ 30.3, 38.8, 48.0, 54.3, 69.5, 74.7, 111.3, 120.8, 125.0, 127.2, 129.4, 129.6, 137.8, 142.3; HRMS (ESI) $[M-H-2Cl]^+$ Calcd for $C_{16}H_{22}N_3O_2$: 288.1712. Found: 288.1705.

4.7.8. (2*R*,4*R*)-2-[2-(4-Chlorophenyl)ethyl]-2-[(1*H*-imidazol-1-yl)methyl]-4-(methoxymethyl)-1,3-dioxolane hydrochloride monohydrate (37)

A solution of sodium methoxide in methanol was prepared by carefully adding sodium (195 mg, 8.48 mmol) to dry methanol (3 mL) under a nitrogen atmosphere, and allowing this solution to cool back to room temperature. This solution was then added to a mixture of (2*R*,4*S*)-2-[2-(4-chlorophenyl)ethyl]-2-[(1*H*-imidazol-1-yl)methyl]-4-[(*p*-toluenesulfonyloxy)methyl]-1,3-dioxolane (**4**)[11] (133 mg, 0.28 mmol) in *N*,*N*-dimethylformamide (2 mL). The mixture was heated at 120 °C with stirring for 7 h. The solution was then concentrated to remove methanol, diluted with a saturated aqueous solution of Na_2CO_3, and extracted with EtOAc (3×). The combined organic extracts were washed sequentially with a saturated aqueous solution of Na_2CO_3, and brine, and then dried (Mg_2SO_4). The solution was concentrated and the golden oily residue purified by flash column chromatography on silica gel (EtOAc) to give the free base as an oil (R_f = 0.13, EtOAc). To a solution of the free base (61 mg, 0.18 mmol, 64%) in warm 2-propanol (2 mL) was added a solution of 37% aqueous HCl (31 mg, 0.31 mmol, 1.7 equiv) in 2-propanol (2 mL); the mixture was concentrated. High-vacuum drying gave **37** (63 mg, 0.17 mmol, 61%) as a white hygroscopic solid: mp 92–93 °C; $[\alpha]_D^{24}$ −11.6 (*c* 0.8 in CD_3OD); ^1H NMR (400 MHz, CD_3OD): δ 1.98 (t, *J* = 8.4 Hz, 2H), 2.69–2.84 (m, 2H), 3.36 (s, 3H), 3.42–3.50 (m, 2H), 3.75 (dd, *J* = 16.0, 8.4 Hz, 1H), 3.76–3.84 (m, 1H), 4.02 (dd, *J* = 7.4, 5.8 Hz, 1H), 4.48 (s, 2H), 7.20 (d, *J* = 8.4 Hz, 2H), 7.27 (d, *J* = 8.4 Hz, 2H), 7.58 (br s, 1H), 7.63 (br s, 1H), 8.96 (br s, 1H); ^{13}C NMR (100 MHz, CD_3OD): δ 29.8, 39.0, 54.7, 59.6, 68.5, 73.5, 77.9, 109.9, 120.5, 125.1, 129.6, 131.0, 132.8, 137.8, 141.5; HRMS (EI) $[M-2H-Cl-O]^+$ Calcd for $C_{17}H_{22}ClN_2O_3$: 337.1319. Found: 337.1306. Anal. Calcd for $C_{17}H_{24}Cl_2N_2O_4$: C, 52.18; H, 6.18; N, 7.16. Found: C, 52.14; H, 5.64; N, 6.96.

4.8. Animals

Liver tissue was obtained from adult male Sprague–Dawley rats (250–300 g) purchased from Charles River Inc. (Montreal, QC, Canada). Rats were cared for in accordance with the principles and guidelines of the Canadian Council on Animal Care and the experimental protocols were approved by Queen's University Animal Care Committee. The animals were maintained on 12-h light cycles and were provided with *ad libitum* access to standard Ralston Purina Laboratory Chow (Ren's Feed Supplies Ltd, Oakville, ON, Canada) and water.

4.9. Preparation of liver microsomal fractions

Microsomal fractions were prepared by differential centrifugation according to previously published methods.[10,30] Briefly, tissue homogenate (15% w/v) was prepared in buffer (20 mM KH_2PO_4, 135 mM KCl, and 0.10 mM EDTA; adjusted to pH 7.4 at 4 °C with 1 M KOH) using a 60S Sonic Dismembrator (Fisher Scientific Ltd, Ottawa, ON, Canada). The homogenate was centrifuged at 10,000 *g* for 20 min at 4 °C, followed by centrifugation of the supernatant at 100,000 *g* for 60 min at 4 °C. The resulting pellet was resuspended in buffer (100 mM KH_2PO_4, 20% v/v glycerol and 1 mM EDTA adjusted to pH 7.4) and stored at −80 °C until use. Protein concentrations were determined by a modification of the Biuret method as described by Marks et al.[31]

4.10. Measurement of CYP2E1 and CYP3A1/3A2 enzymatic activity

In order to determine the in vitro CYP2E1 and CYP3A1/3A2 enzymatic activities, acetone-treated and dexamethasone-treated Sprague–Dawley rats were used, respectively. An acetone solution (5% v/v) was provided in place of water for 3 days. Dexamethasone-5 (Vetoquinol Canada Inc, Lavaltrie, QC, Canada) was injected i.p. (15 mg/kg/day for 3 days). The animals were sacrificed by decapitation and the livers perfused. Microsomes were prepared according to the procedures outlined above. CYP2E1 hydroxylation of *p*-nitrophenol was determined by the spectrophotometric measurement of 4-nitrocatechol.[32] CYP3A1/3A2-catalyzed erythromycin *N*-demethylase activity was determined by the spectrophotometric measurement of formaldehyde.[33,34] Briefly, reaction mixtures (500 μL) consisting of 100 mM phosphate buffer (pH 7.4), 100 μM *p*-nitrophenol (CYP2E1) or 400 μM erythromycin (CYP3A1/3A2), 2 mg/mL protein, and inhibitors were pre-incubated for 10 min at 37 °C. Reactions were initiated by adding NADPH at a final concentration of 1 mM and were incubated for an additional 30 min (CYP2E1) or 60 min (CYP3A1/3A2) at 37 °C. Reactions were stopped upon the addition of perchloric acid (0.6 N or 22% for CYP2E1 or CYP3A1/3A2, respectively). The effects of the HO inhibitors on enzyme activity were tested at concentrations in the range of 0.01–100 μM.

4.11. In vitro HO activity assay

HO activity in rat spleen and brain microsomal fractions was determined by the quantitation of CO formed from the degradation of methemalbumin (heme complexed with albumin).[35,36] Spleen and brain (Sprague–Dawley rats) microsomal fractions were prepared according to the procedure outlined by Appleton et al.[30] Protein concentration of microsomal fractions was determined by a modification of the biuret method.[36] Incubations for HO activity analysis were done under conditions for which the rate of CO formation (pmol CO × min^{-1} × mg $protein^{-1}$) was linear with respect to time and microsomal protein concentration. Briefly, reaction mixtures (150 μL) consisting of 100 mM phosphate buffer (pH 7.4), 50 μM methemalbumin, and 1 mg/mL protein were pre-incubated with the inhibitors at final concentrations ranging from 0.1 to 100 μM for 10 min at 37 °C. Reactions were initiated by adding NADPH at a final concentration of 1 mM and incubations were performed for an additional 15 min at 37 °C. Reactions were stopped by instantly freezing the reaction mixture on dry ice, and CO formation was monitored by gas chromatography according to the method described by Vreman and Stevenson.[35]

4.12. Analysis of enzyme inhibition

The data resulting from the above experiments were plotted as non-linear regression (sigmoidal dose–response) curves using GRAPHPAD Prism (Version 3). The values on the abscissa represent the logarithm of inhibitor concentration (in μM), whereas the values of the activity on the ordinate are expressed as a percentage of the control experiments without inhibitor. From these curves, the value of the concentration (EC_{50}) of the inhibitor at which the enzyme's activity is halfway between the bottom and top plateau of the curve, as well as the top and the bottom plateau values of the curves, have been retrieved using the same program, and input into the following

formula to give the calculated values of the concentration (IC_{50}) of the compound under evaluation for which the activity of the enzyme was inhibited by 50% compared to the control.

$$IC_{50} = \frac{EC_{50}}{\frac{bottom-top}{50-top} - 1}.$$

The IC_{50} value reported for each compound is the mean of the values recorded in replicate experiments, and for each of these replicate experiments (consisting of two separate assays) an individual IC_{50} value was calculated in the manner described. The IC_{50} values for the replicate experiments were employed to generate the reported standard deviation value.

4.13. Molecular modeling of compound 3 in the binding site of hHO-1

An initial template of hHO-1 was based on the x-ray crystallographic structure of hHO-1 in complex with 1-(adamantan-1-yl)-2-(1*H*-imidazol-1-yl)ethanone (PDB 3CZY) from which the inhibitor had been omitted.[22] An initial template of inhibitor **3** was generated using CS CHEM3D ULTRA (version 6) and the Dundee PRODRG2 Server.[37] Inhibitor **3** was then manually inserted into the inhibitor binding site of hHO-1 using XFit in the CCP4 suite.[38] The previously published structure of hHO-1 into which azalanstat had been docked was utilized as a guide.[22] To compare binding of the inhibitor to hHO-2, residues within the inhibitor binding site of hHO-1 were changed to the corresponding residues of hHO-2[23] using either XFit or PYMOL.[39] Analyses of contact distances between the two HO structures and the docked inhibitor, as well as image preparation, were performed using PYMOL.

Acknowledgments

The authors thank the Canadian Institutes of Health Research for a grant-in-aid from the Canadian Institutes of Health Research (MOP 64305), and Tracy Gifford, Brian McLaughlin, and Dragic Vukomanovic for assistance with the biological evaluations.

References and notes

1. Maines, M. D. *Ann. Rev. Pharmacol. Toxicol.* **1997**, *37*, 517.
2. Vreman, H. J.; Wong, R. J.; Stevenson, D. K. In *Carbon Monoxide and Cardiovascular Function*; Wang, R. J., Ed.; CRC Press: Boca Raton, 2002; p 273.
3. Mancuso, C. *Antiox. Redox Signal.* **2004**, *6*, 878.
4. Ndisang, J. F.; Tabien, H. E.; Wang, R. *J. Hypertens.* **2004**, *22*, 1057.
5. Ryter, S. W.; Otterbein, L. E.; Morse, D.; Choi, A. M. *Mol. Cell. Biochem.* **2002**, *234–235*, 249.
6. Akagi, R.; Takahashi, T.; Sassa, S. *Contrib. Nephrol.* **2005**, *148*, 70.
7. Abraham, N. G.; Kappas, A. *Free Radical Biol. Med.* **2005**, *39*, 1.
8. Takeda, A.; Itoyama, Y.; Kimpara, T.; Zhu, X.; Avila, J.; Dwyer, B. E.; Perry, G.; Smith, M. A. *Antioxid. Redox Signal.* **2004**, *6*, 888.
9. Fang, J.; Akaike, T.; Maeda, H. *Apoptosis* **2004**, *9*, 27.
10. Kinobe, R. T.; Vlahakis, J. Z.; Vreman, H. J.; Stevenson, D. K.; Brien, J. F.; Szarek, W. A.; Nakatsu, K. *Br. J. Pharmacol.* **2006**, *147*, 307.
11. Vlahakis, J. Z.; Kinobe, R. T.; Bowers, R. J.; Brien, J. F.; Nakatsu, K.; Szarek, W. A. *Bioorg. Med. Chem. Lett.* **2005**, *15*, 1457.
12. Vlahakis, J. Z.; Kinobe, R. T.; Bowers, R. J.; Brien, J. F.; Nakatsu, K.; Szarek, W. A. *J. Med. Chem.* **2006**, *49*, 4437.
13. Roman, G.; Riley, J. G.; Vlahakis, J. Z.; Kinobe, R. T.; Brien, J. F.; Nakatsu, K.; Szarek, W. A. *Bioorg. Med. Chem. Lett.* **2007**, *15*, 3225.
14. Tani, K.; Suwa, K.; Tanigawa, E.; Ise, T.; Yamagata, T.; Tatsuno, Y.; Otsuka, S. *J. Organomet. Chem.* **1989**, *370*, 203.
15. Grotenbreg, G. M.; Kronemeijer, M.; Timmer, M. S. M.; El Oualid, F.; van Well, R. M.; Verdoes, M.; Spalburg, E.; van Hooft, P. A. V.; de Neeling, A. J.; Noort, D.; van Boom, J. H.; van der Marel, G. A.; Overkleeft, H. S.; Overhand, M. *J. Org. Chem.* **2004**, *69*, 7851.
16. Gartiser, T.; Selve, C.; Delpuech, J.-J. *Tetrahedron Lett.* **1983**, *24*, 1609.
17. Maines, M. D. *FASEB J.* **1988**, *2*, 2557.
18. Xia, Z. W.; Cui, W. J.; Zhang, X. H.; Shen, Q. X.; Wang, J.; Li, Y. Z.; Chen, S. N.; Yu, S. C. *World J. Gastroenterol.* **2002**, *8*, 1123.
19. Trakshel, G. M.; Kutty, R. K.; Maines, M. D. *Arch. Biochem. Biophys.* **1988**, *260*, 732.
20. Vreman, H. J.; Cipkala, D. A.; Stevenson, D. K. *Can. J. Physiol. Pharmacol.* **1996**, *74*, 278.
21. Ortiz de Montellano, P. R. In *Cytochrome P-450: Structure, Mechanism and Biochemistry*; Ortiz de Montellano, P. R., Ed.; Plenum Press: New York, 1986.
22. Rahman, M. N.; Vlahakis, J. Z.; Szarek, W. A.; Nakatsu, K.; Jia, Z. *J. Med. Chem.* **2008**, *51*, 5943.
23. Bianchetti, C. M.; Yi, L.; Ragsdale, S. W.; Phillips, G. N., Jr. *J. Biol. Chem.* **2007**, *282*, 37624.
24. Lad, L.; Schuller, D. J.; Shimizu, H.; Friedman, J.; Li, H.; Ortiz de Montellano, P. R.; Poulos, T. L. *J. Biol. Chem.* **2003**, *278*, 7834.
25. Schuller, D. J.; Wilks, A.; Ortiz de Montellano, P. R.; Poulos, T. L. *Nat. Struct. Biol.* **1999**, *6*, 860.
26. Sugishima, M.; Higashimoto, Y.; Oishi, T.; Takahashi, H.; Sakamoto, H.; Noguchi, M.; Fukuyama, K. *Biochemistry* **2007**, *46*, 1860.
27. Yi, L.; Ragsdale, S. W. *J. Biol. Chem.* **2007**, *282*, 21056.
28. Gottlieb, H. E.; Kotlyar, V.; Nudelman, A. *J. Org. Chem.* **1997**, *62*, 7512.
29. Vlahakis, J. Z.; Kinobe, R. T.; Nakatsu, K.; Szarek, W. A.; Crandall, I. E. *Bioorg. Med. Chem. Lett.* **2006**, *16*, 2396.
30. Appleton, S. D.; Chretien, M. L.; McLaughlin, B. E.; Vreman, H. J.; Stevenson, D. K.; Brien, J. F.; Nakatsu, K.; Maurice, D. H.; Marks, G. S. *Drug Metab. Dispos.* **1999**, *27*, 1214.
31. Marks, G. S.; McLaughlin, B. E.; Vreman, H. J.; Stevenson, D. K.; Nakatsu, K.; Brien, J. F.; Pang, S. C. *J. Cardiovasc. Pharmacol.* **1997**, *30*, 1.
32. Koop, D. R. *Mol. Pharmacol.* **1986**, *29*, 399.
33. Nash, T. *Biochem. J.* **1953**, *55*, 416.
34. Kim, H.; Putt, D. A.; Zangar, R. C.; Wolf, R.; Guengerich, F. P.; Edwards, R. J.; Hollenberg, P. F.; Novak, R. F. *Drug Metab. Dispos.* **2001**, *29*, 353.
35. Vreman, H. J.; Stevenson, D. K. *Anal. Biochem.* **1988**, *168*, 31.
36. Cook, M. N.; Nakatsu, K.; Marks, G. S.; McLaughlin, B. E.; Vreman, H. J.; Stevenson, D. K. *Can. J. Physiol. Pharmacol.* **1995**, *73*, 515.
37. Schuettelkopf, A. W.; van Aalten, D. M. F. *Acta Crystallogr., Sect. D* **2004**, *60*, 1355.
38. Collaborative Computational Project, Number 4. The CCP4 Suite: Programs for Protein Crystallography. *Acta Crystallogr., Sect. D* **1994**, *50*, 760.
39. DeLano, W. L. *The PYMOL Molecular Graphics System, Version 0.99rc6*; Delano Scientific: Palo Alto, CA, 2002.